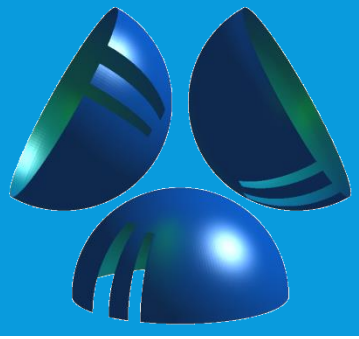

# Black Holes Everywhere

**Omar López-Cruz**

**omarlx@inaoep.mx**

*Instituto Nacional de Astrofísica, Optica y Electrónica*
*(INAOE), Puebla, México*

*XXXI Reunión Annual de la División de Partículas y Campos, SMF*

# SUMMARY

In this talk we highlight the role of black holes in the universe.

I present projects currently underway where the importance of black holes become apparent.

# EMPIRICAL CORRELATION

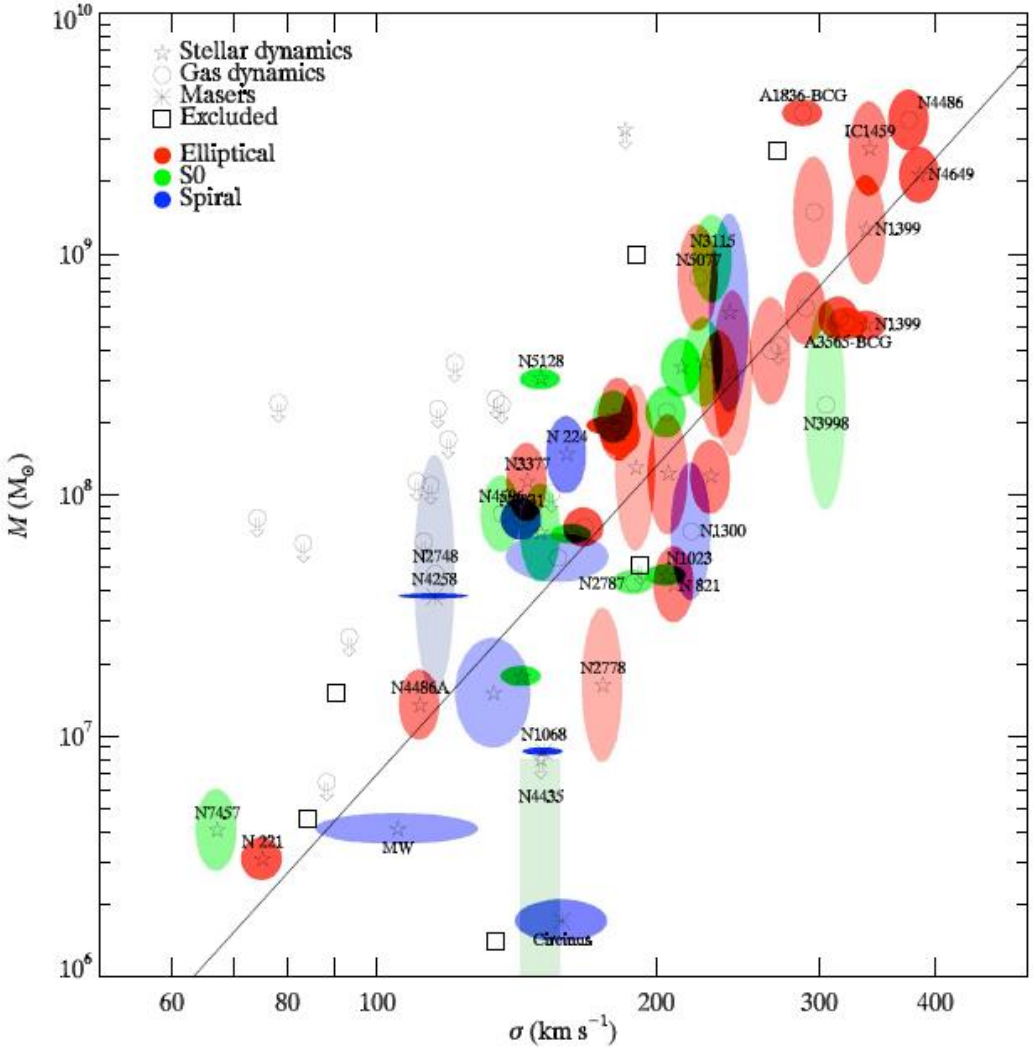


$$\sigma \sim M_\bullet$$

# WE BEGIN WITH SUPERMASSIVE BLACK HOLES.

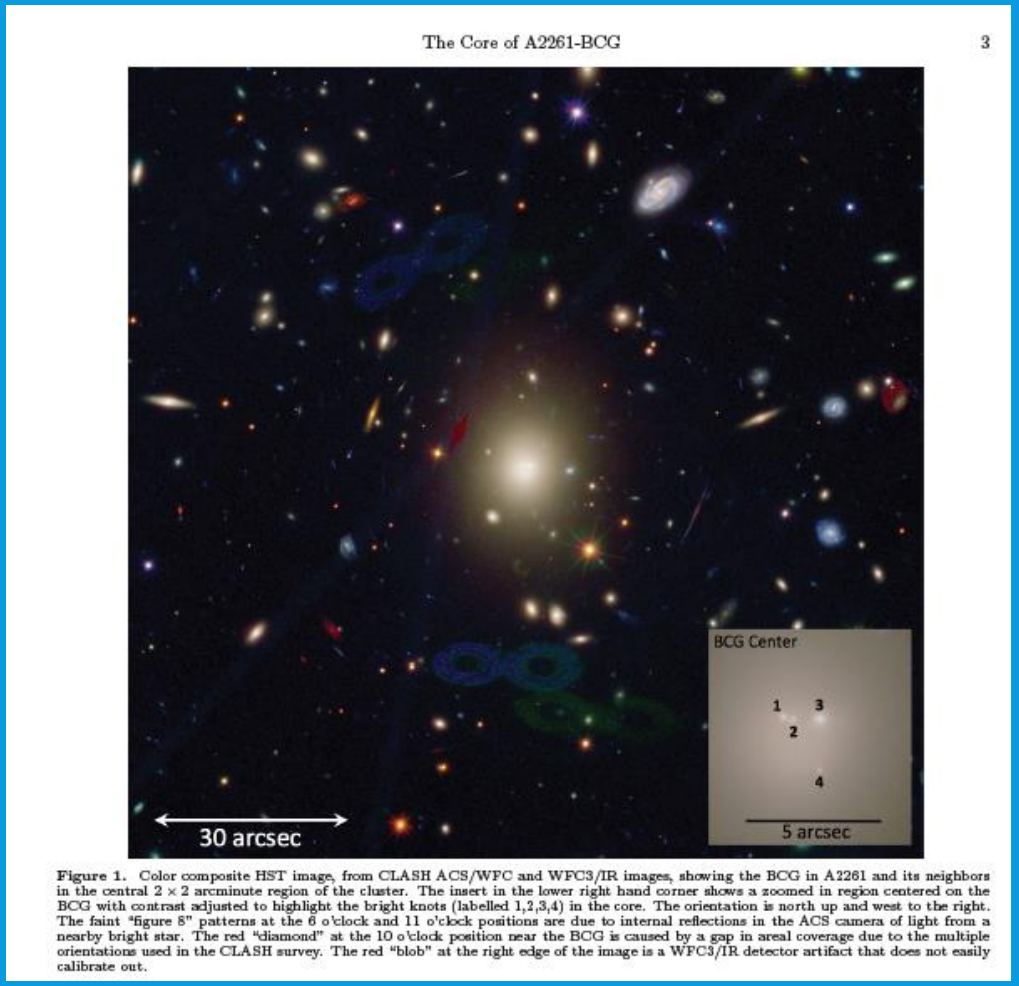


Figure 1. Color composite HST image, from CLASH ACS/WFC and WFC3/IR images, showing the BCG in A2261 and its neighbors in the central 2 × 2 arcminute region of the cluster. The insert in the lower right hand corner shows a zoomed in region centered on the BCG with contrast adjusted to highlight the bright knots (labelled 1,2,3,4) in the core. The orientation is north up and west to the right. The faint "figure 8" patterns at the 6 o'clock and 11 o'clock positions are due to internal reflections in the ACS camera of light from a nearby bright star. The red "diamond" at the 10 o'clock position near the BCG is caused by a gap in areal coverage due to the multiple orientations used in the CLASH survey. The red "blob" at the right edge of the image is a WFC3/IR detector artifact that does not easily calibrate out.

A2261-BGC

z=0.2233

$\alpha_{2000}$=17:22:27.18

$\delta_{2000}$=+32:07:57.1

$$M_{2500} = (2.9 \pm 0.5) \times 10^{14}\ M_{\odot}$$

# POSTMAN ET AL. 2012 WERE INTRODUCING THE LARGEST CORE YET DETECTED IN ANY GALAXY…

details

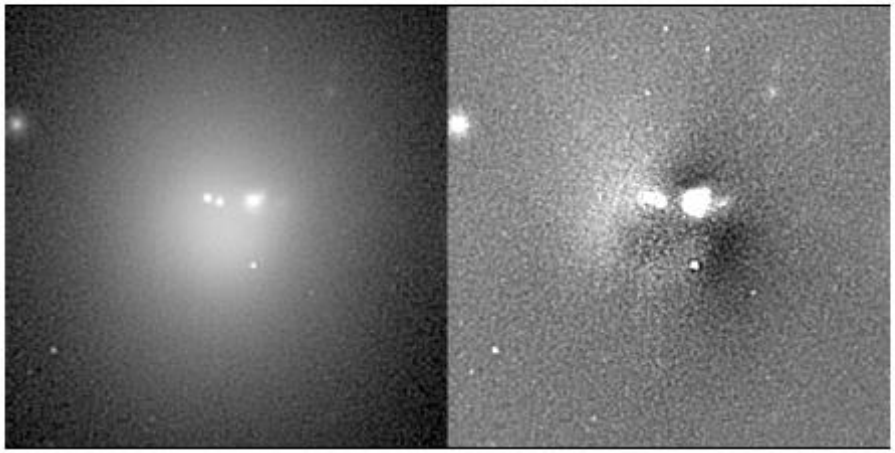

**Figure 3.** The left panel shows the center of the F814W image of the BCG after Lucy (1974)-Richardson (1972) deconvolution. The region shown is $12'' \times 12''$; ($43.2 \times 43.2$ kpc) the intensity scale is logarithmic. North is at the top and east to the left. The right panel shows the residuals after subtraction of a model reconstructed from the surface photometry of the BCG. The over all structure of the residuals is a dipole pattern of positive residuals NE of the core and negative residuals to the SW. This suggests that the core is slightly displaced from the surrounding envelope in the SW direction.

The Core o

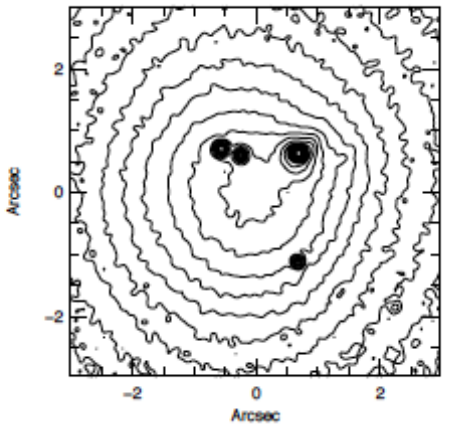


**Figure 4.** A contour plot of the core of A2261-BCG. The contour levels have an arbitrary zeropoint, but are spaced by 0.25 mag in surface brightness. North is to the top and east to the left. Note that the contour levels are closer together in the SW direction outside the core than they are in the NE, supporting the dipole-like residual pattern seen in Figure 3 and the conclusion that the core is displaced to the SW relative to the envelope center.

# THE NUKER LAW (LAUER ET AL. 1995)

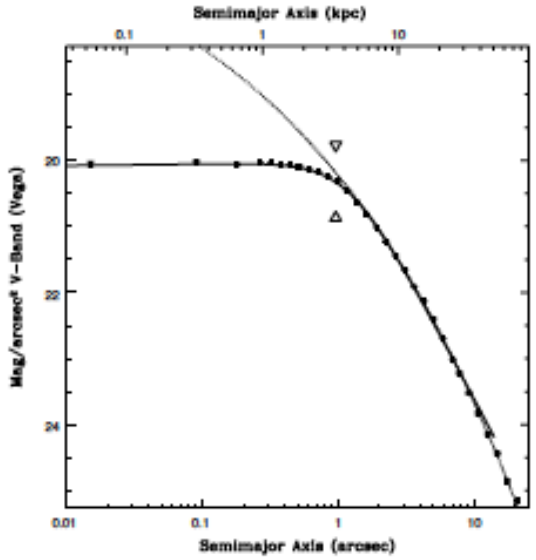


**Figure 5.** The central surface brightness profile of A2261-BCG as measured (solid points) is shown with two "Nuker-law" profile fits (Lauer et al. 1995). The error bars are smaller than the points, but for the central few measurements. For comparison to previous studies the profile is normalized to $z = 0$ V-band (Vega). The solid line is the best-fitting Nuker-law and features a slightly depressed ($\gamma = -0.01$) cusp as $r \to 0$. The dotted line is an is an $r^{1/4}$-law (an $n = 4$ Sérsic-law) fitted to the envelope. The triangles indicate the cusp-radius.

$$I(r) = 2^{(\beta-\gamma)/\alpha} I_b \left(\frac{r_b}{r}\right)^{\gamma} \left[1 + \frac{r}{r_b}\right]^{(\gamma-\beta)/\alpha}$$

$$r_\gamma \equiv r_b \left(\frac{1/2 - \gamma}{\beta - 1/2}\right)^{1/\alpha}$$

$$\gamma = -0.01,\ \beta = 1.56,\ \alpha = 2.41 \pm 0.18,\ r_b = 1.2''$$

$$r_\gamma = 0''.89 \pm 0''.02;\ 3.2 \pm 0.1\mathrm{kpc}$$

# LUMINOSITY VS. CUSP RADIUS



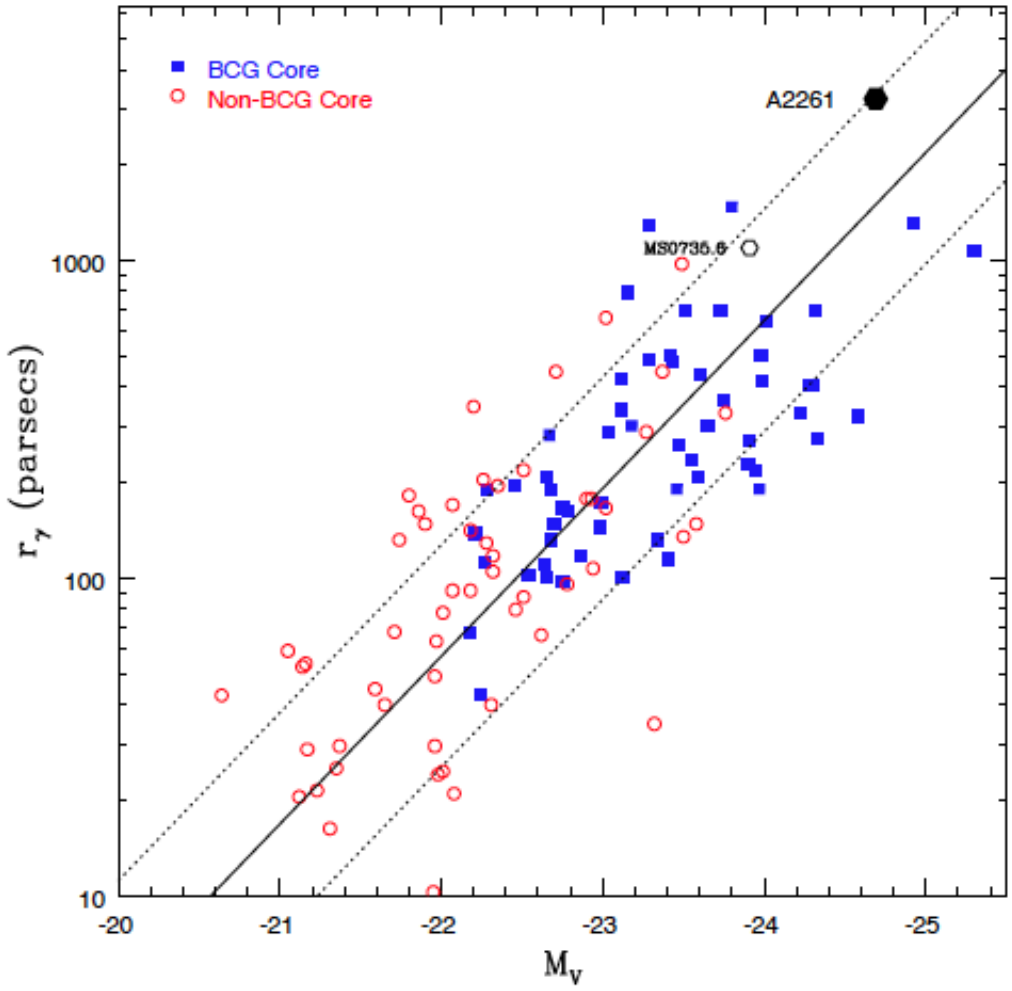


**Figure 7.** The relationship between cusp-radius and total galaxy luminosity (V-band Vega-based). The galaxy sample plotted was assembled in Lauer et al. (2007a) from a variety of sources (the figure is adopted from Figure 5 in that paper). The BCGs in particular come from the Laine et al. (2002) sample. The Lauer et al. (2007a) $r_\gamma - L$ relationship (also given in equation 4) is plotted; the dotted lines indicate $\pm 1\sigma$ scatter about the mean relationship. A2261-BCG is plotted at the top, clearly has a cusp-radius larger than all other galaxies in the sample. The large core in the MS0735.6+7421 BCG discovered by McNamara et al. (2009) is also plotted for comparison.

# BUT, I RECALLED ABELL 85. JAMES P. BROWN AND I HAVE WORKED ON IT BACK IN 1995 AT DA&A, UOFT

LOCOS, *BRI* images,

Taken with the KPNO 0.9m Telescope using the T2KA CCD. Seeing ~1.6 arcsec

Scale 0.68 arcsec/pixel
$z=0.05529 +/- 2.4 \times 10^{-4}$

Hoessel and collaborators during the early 80's have already singled out that that HOLM 015A had a very large core (modified Hubble Profile)

# WE TRIED DGCG ON A85

We tried DGCG on A85 using the Nuker Law.

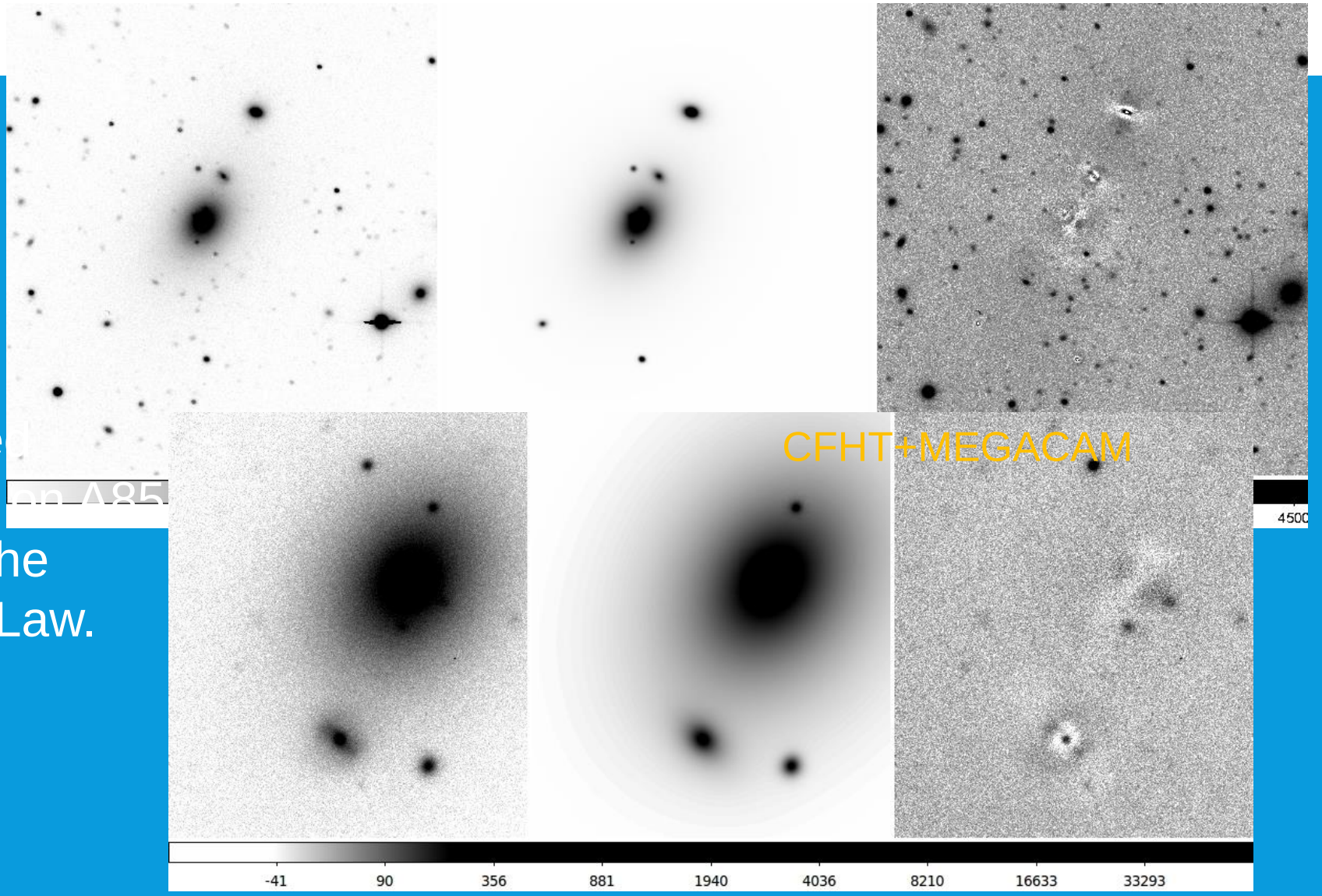

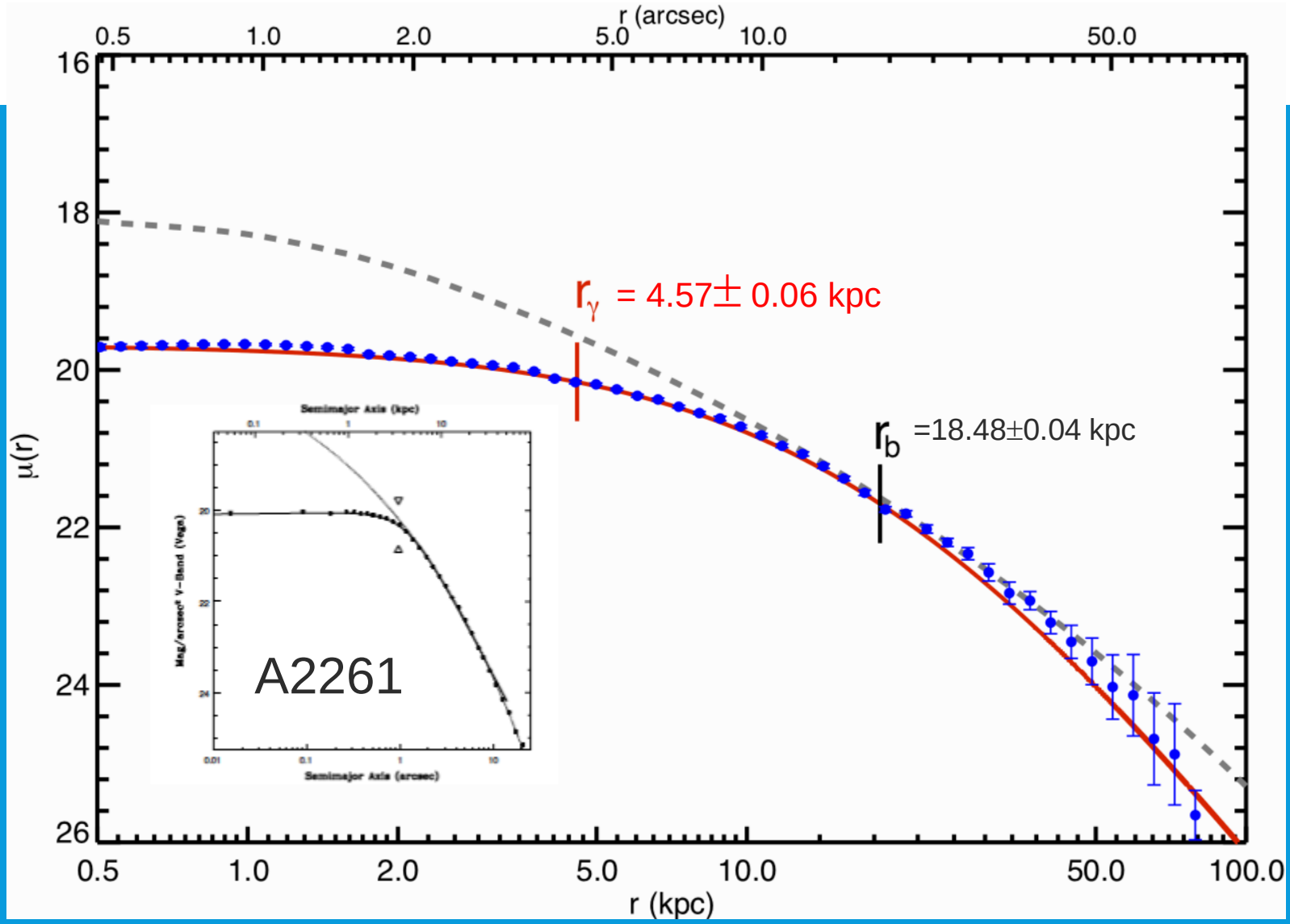
r (arcsec)
0.5
1.0
2.0
5.0
10.0
50.0
16
18
20
22
24
26
μ(r)
$r_\gamma$ = 4.57± 0.06 kpc
$r_b$ =18.48±0.04 kpc
A2261
Semimajor Axis (kpc)
Semimajor Axis (arcsec)
0.5
1.0
2.0
5.0
10.0
50.0
100.0
r (kpc)

# THE LARGEST CORE KNOWN SO FAR!!!

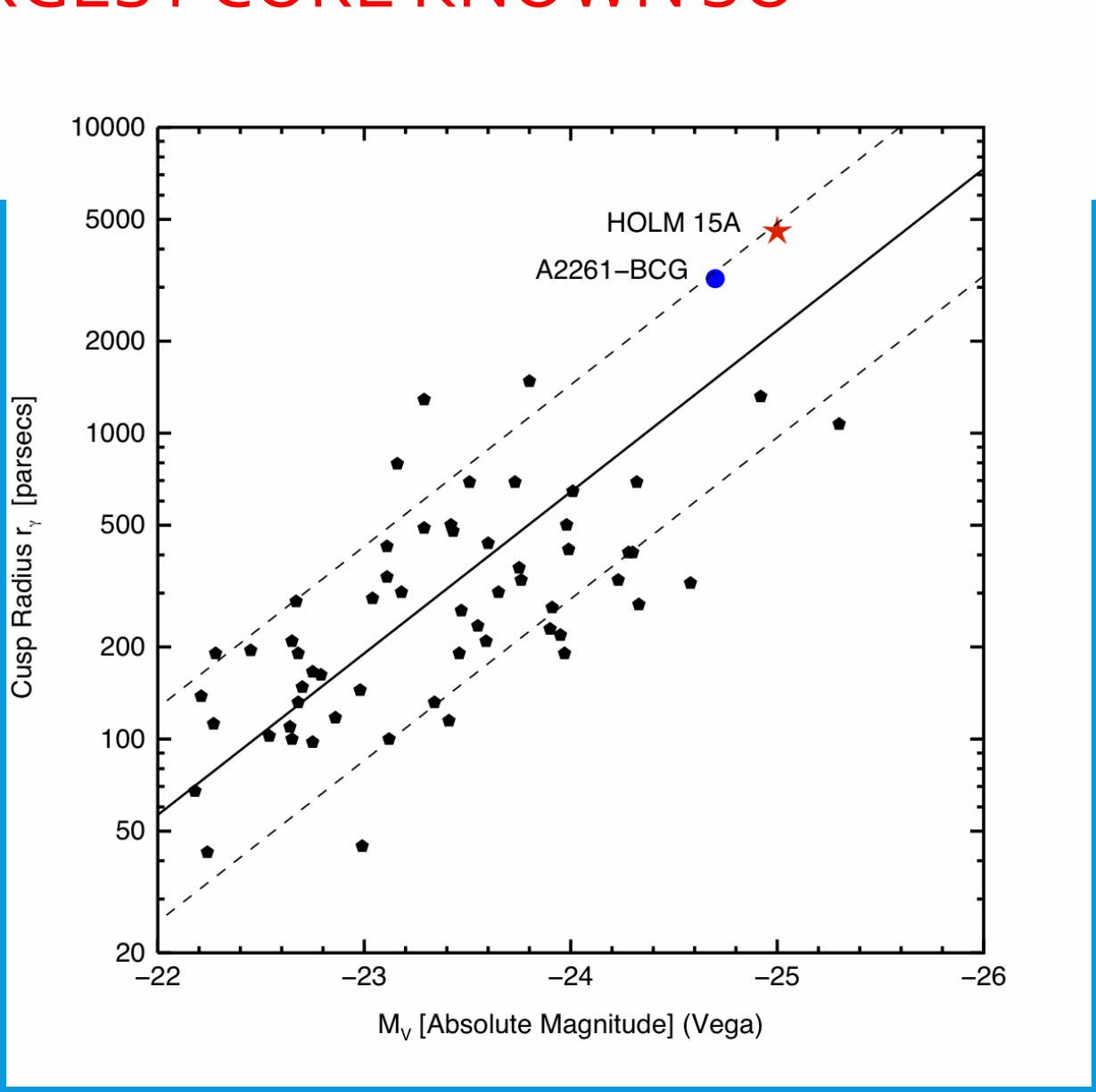

# HOW BIG IS THE SMBH IN HOLM 15A?

Table 2. Holm 15A: Black Hole Mass Estimates

| Relation | $M_\bullet$ [$M_\odot$] | Reference |
|---|---|---|
| $M_\bullet - \sigma$ | $\sim 2.1 \times 10^9$ | Kormendy & Ho (2013, Eqs. 6) |
| $M_\bullet - L_{K,bulge}$* | $\sim 9.2 \times 10^9$ | Kormendy & Ho (2013, Eqs. 7) |
| $M_\bullet - L_{V,def}$ | $\sim 2.6 \times 10^{11}$ | Kormendy & Bender (2009, Eq. 3) |
| $M_\bullet - r_b$ | $\sim 1.7 \times 10^{11}$ | Rusli et al. (2013, Eq. 13) |
| $M_\bullet - r_\gamma$ | $\sim 3.1 \times 10^{11}$ | Lauer et al. (2007, Eq. 26 ) |

*Taking the entire galaxy as a classical bulge, and correcting the value of $H_0$

$M_\bullet \sim 9 \times 10^{10}\ M_\odot$

# WHAT IS THE EXPECTED MASS FOR THE CLUSTER'S DARK MATTER HALO?

$$\frac{\mathrm{M}_\bullet}{10^8 \mathrm{M}_\odot} = 0.168 \left( \frac{V_{circ}}{200\ \mathrm{km\,s^{-1}}} \right)^{5.45}$$

$\sigma_{cl} = 752 \pm 34\ \mathrm{km\,s^{-1}},\ V_{circ} = \sqrt{2}\sigma_{cl};$

hence, the mass of the SMBH for Abell 85 DM halo is :

$$\mathrm{M}_\bullet \sim 1.5 \times 10^{11}\ \mathrm{M}_\odot$$

# ARE JOINING THE STUPIDITY PANDEMIC?

Mayebe not

SMBH dominate the entropy budget in the observable universe (Egan & Lineweaver 2010)

$$S_{\mathrm{SMBH}} = 3.1^{+3.0}_{-1.7} \times 10^{104}\ k$$

Each SMBH contributes

$$S_{\mathrm{BH}} = \frac{kc^3}{G\hbar}\frac{A}{4} = \frac{4\pi kG}{c\hbar}M_\bullet^2$$

Bekenstein (1973), Hawking (1966)

$$A = \frac{16\pi G^2 M_\bullet^2}{c^4}$$

# EL PAÍS, SPAIN'S LARGEST NEWSPAPER

## Descubierto el mayor agujero negro supermasivo del universo cercano

El proyecto fue liderado por el investigador mexicano Omar López-Cruz

LAURA DELLE FEMMINE | México | 17 OCT 2014 - 05:12 CEST 3

Archivado en: Agujeros negros Astrofísica Galaxias México Norteamérica Latinoamérica Universo América Astronomía Ciencia

Ilustración de un aquejero negro. / NASA

Son objetos que no se detectan directamente, existen gracias a estudios teóricos y hasta infringen principios de la física. Aunque todavía quede mucho por conocer acerca de los agujeros negros —concentraciones de materia con un campo gravitacional capaz de atrapar a cualquier partícula, hasta a los fotones (luz)—, un equipo liderado por el astrofísico mexicano Omar López-Cruz ha anunciado este jueves haber descubierto al más grande del universo conocido, es decir, hasta 2.000 millones de años luz.




DAILY NEWS 6 November 2014

# Giant galactic core formed after black hole battle

By **Hal Hodson**

The largest galactic core ever seen may be the remnant of a battle for black hole supremacy.

Omar Lopez-Cruz of Mexico's National Institute of Astrophysics, Optics and Electronics and his team measured the core of galaxy Holm 15A, 650 million light years from Earth. They found it was a record-breaking 15,000 light years across – about one-sixth the diameter of the entire Milky Way.

When two galaxies merge, their central black holes start to orbit each other as a binary system. Nearby stars get slung out of their orbits away from the core. This steals energy from the black hole binary and extends the size of the core, making it more diffuse. Eventually, the black holes merge.

Holm 15A's core's size suggests the black hole it hosts could weigh 100 billion times the mass of our sun – nearly as much as the Milky Way. If so, it probably formed as two or three separate black holes jostled for position before merging into one, puffing up Holm 15A's core in the process.

**Journal reference:** *Astrophysical Journal Letters*, DOI: 10.1088/2041-8205/795/2/L31

# BONFINI ET AL. (2015) HAS CHALLENGED OUR RESULT.

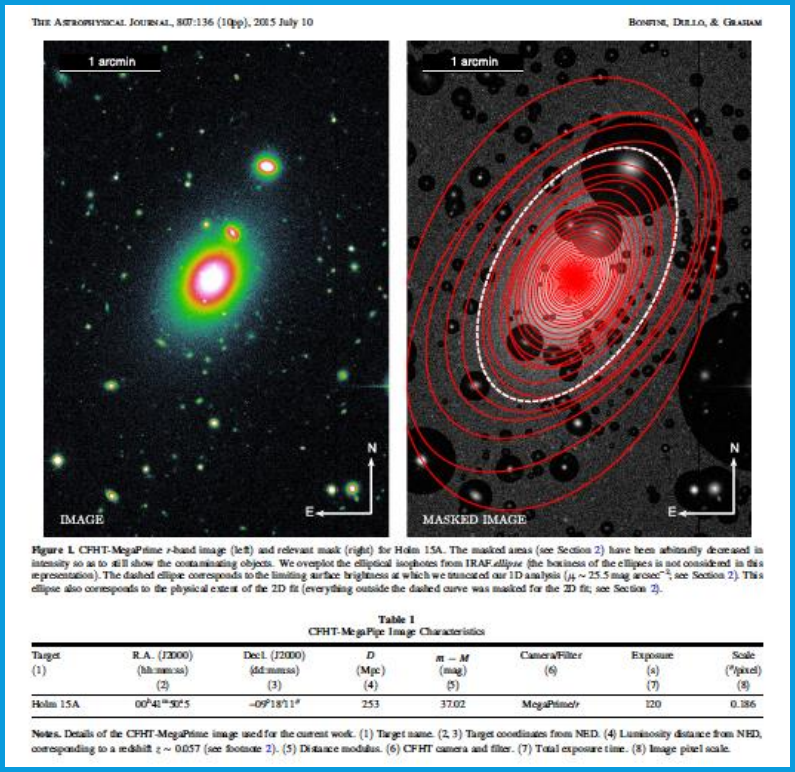


**Figure 1.** CFHT-MegaPrime *r*-band image (left) and relevant mask (right) for Holm 15A. The masked areas (see Section 2) have been arbitrarily decreased in intensity so as to still show the contaminating objects. We overplot the elliptical isophotes from IRAF *ellipse* (the boxiness of the ellipses is not considered in this representation). The dashed ellipse corresponds to the limiting surface brightness at which we truncated our 1D analysis ($\mu_r \sim 25.5$ mag arcsec$^{-2}$; see Section 2). This ellipse also corresponds to the physical extent of the 2D fit (everything outside the dashed curve was masked for the 2D fit; see Section 2).

**Table 1**
CFHT-MegaPipe Image Characteristics

| Target (1) | R.A. (J2000) (hh:mm:ss) (2) | Decl. (J2000) (dd:mm:ss) (3) | $D$ (Mpc) (4) | $m-M$ (mag) (5) | Camera/Filter (6) | Exposure (s) (7) | Scale ("/pixel) (8) |
|---|---|---|---|---|---|---|---|
| Holm 15A | $00^h41^m50^s.5$ | $-09°18'11''$ | 253 | 37.02 | MegaPrime/*r* | 120 | 0.186 |

Notes. Details of the CFHT-MegaPrime image used for the current work. (1) Target name. (2, 3) Target coordinates from NED. (4) Luminosity distance from NED, corresponding to a redshift $z \sim 0.057$ (see footnote 2). (5) Distance modulus. (6) CFHT camera and filter. (7) Total exposure time. (8) Image pixel scale.

Core-Sérsic: Trujillo et al (2004)et al. (2004)

$$I(R) = I' \left[1 + \left(\frac{R_b}{R}\right)^{\alpha}\right]^{\frac{\gamma}{\alpha}} \exp\left(-b\left[\frac{R^{\alpha} + R_b^{\alpha}}{R_e^{\alpha}}\right]^{\frac{1}{\alpha n}}\right)$$

$$I' = I_b 2^{\frac{\gamma}{\alpha}} exp\left(b\left[\frac{2^{\frac{1}{\alpha}} R_b}{R_e}\right]^{\frac{1}{n}}\right)$$

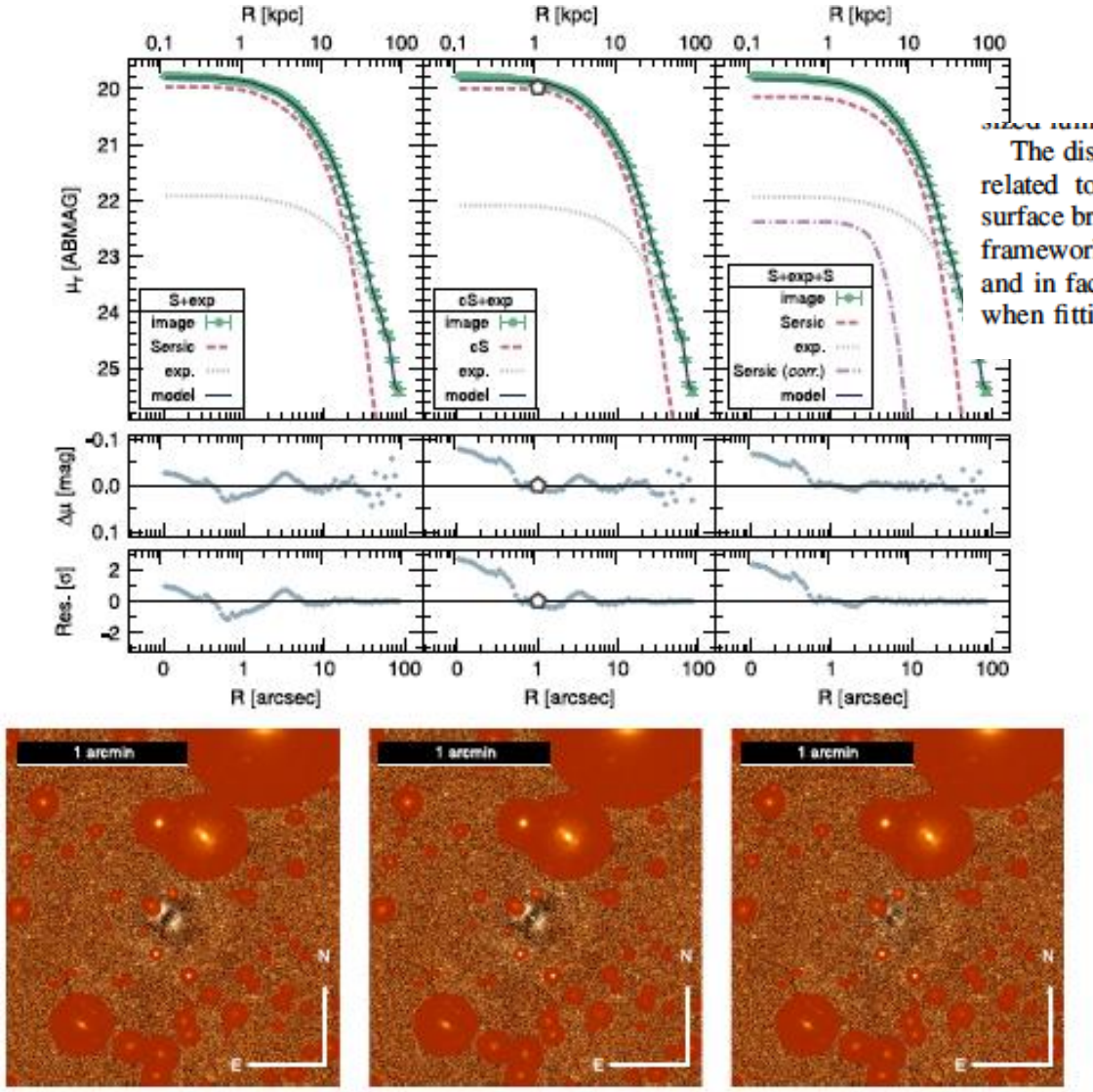


**Figure 4.** 2D image analysis: results of the fits to the 2D image of Holm 15A performed assuming a Sérsic+exponential model (left); a core-Sérsic +exponential model (middle); and a Sérsic+exponential model plus an additional inner Sérsic component intended to compensate for the single ellipticity of the 2D model components (right). Top. The green data points represent the major-axis surface brightness profile measured over the isophotes defined using IRAF.*ellipse* (i.e., the same measurement presented in Figure 2). The curves represent the surface brightness profile of the model images measured over exactly the same isophotes. The continuous curves show the global models, while the dashed curves represent their sub-components. We stress that these are *not* fits to the 1D profile, but rather surface brightness measurements (projections) of the 2D models. The pentagon indicates the location of the core-Sérsic model's break radius. The panels underneath the profiles represent the data residuals about the fitted models, first expressed in terms of the difference in surface brightness, and then in terms of residuals (in units of counts) divided by the standard deviation as measured on the "sigma" image. Bottom. The actual residual images that were minimized by GALFIT-CORSAIR. Masked objects are highlighted as in Figure 1.

The discrepancies between our results and those of LC14 are related to the adopted paradigm for the description of the surface brightness distribution, i.e., the core-Sérsic or the Nuker framework. There is no formal mistake in the analysis of LC14, and in fact we were able to reproduce their Nuker parameters when fitting a Nuker model in 2D with GALFIT. However, for

Bonfini et al. (2015) used GALFIT-CORSAIR and showed that Core-Sérsic profile doesn´t work for Holm 15A, but recovered Lópe-Cruz et al. (2014) Nuker fit.

# MADRID & DONZELLI (2016) HAVE ALSO CHALLENGED OUR RESULT.

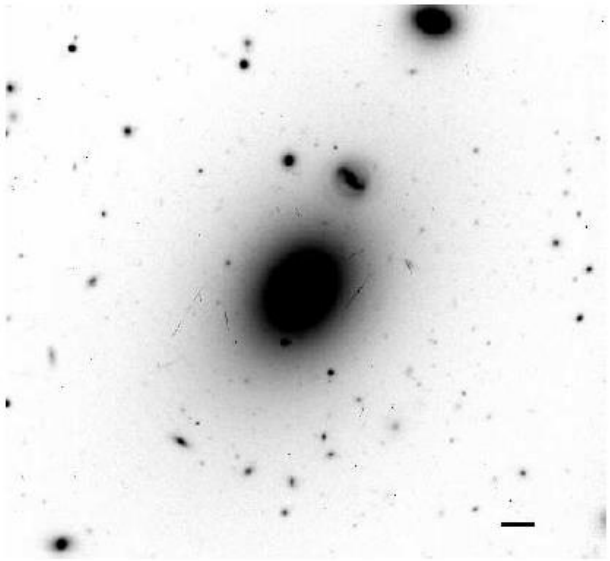

FIG. 1.— Gemini Multi Object Spectrograph image of Abell 85 The scale bar on the lower right represents a length of 10 kpc North is up and east is left.

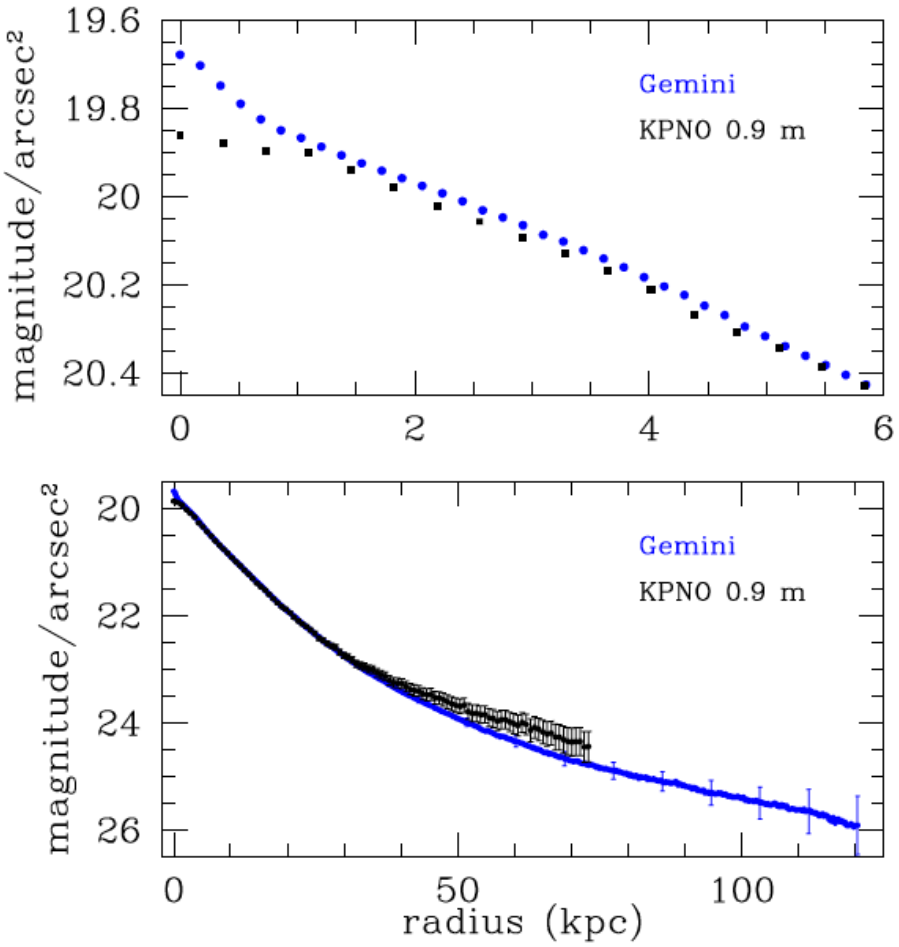

# HOLM 15A VS. A GIANT ELLIPTICAL

If it is not a core then what is it?

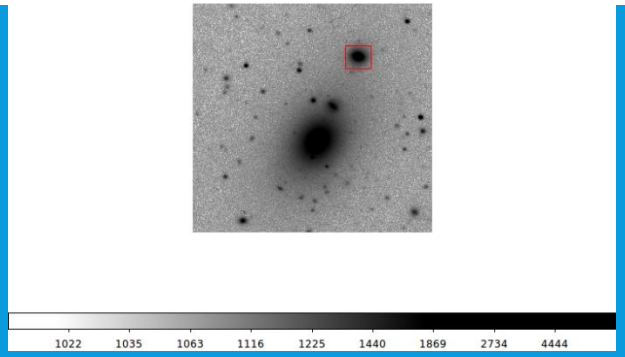


Nobody denies that $10^{10}$ $M_{sun}$ lurks in the core Holm 15A.

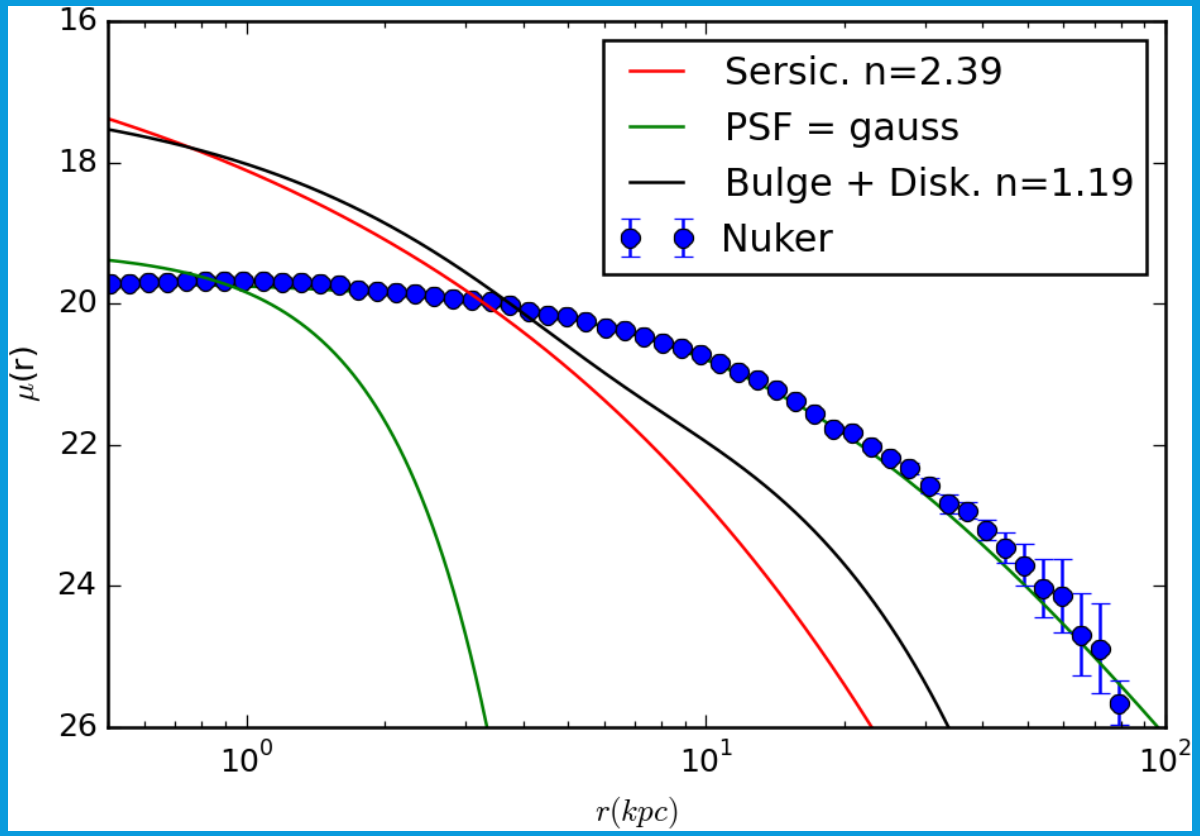

# IS THERE A SMBH BINARY?

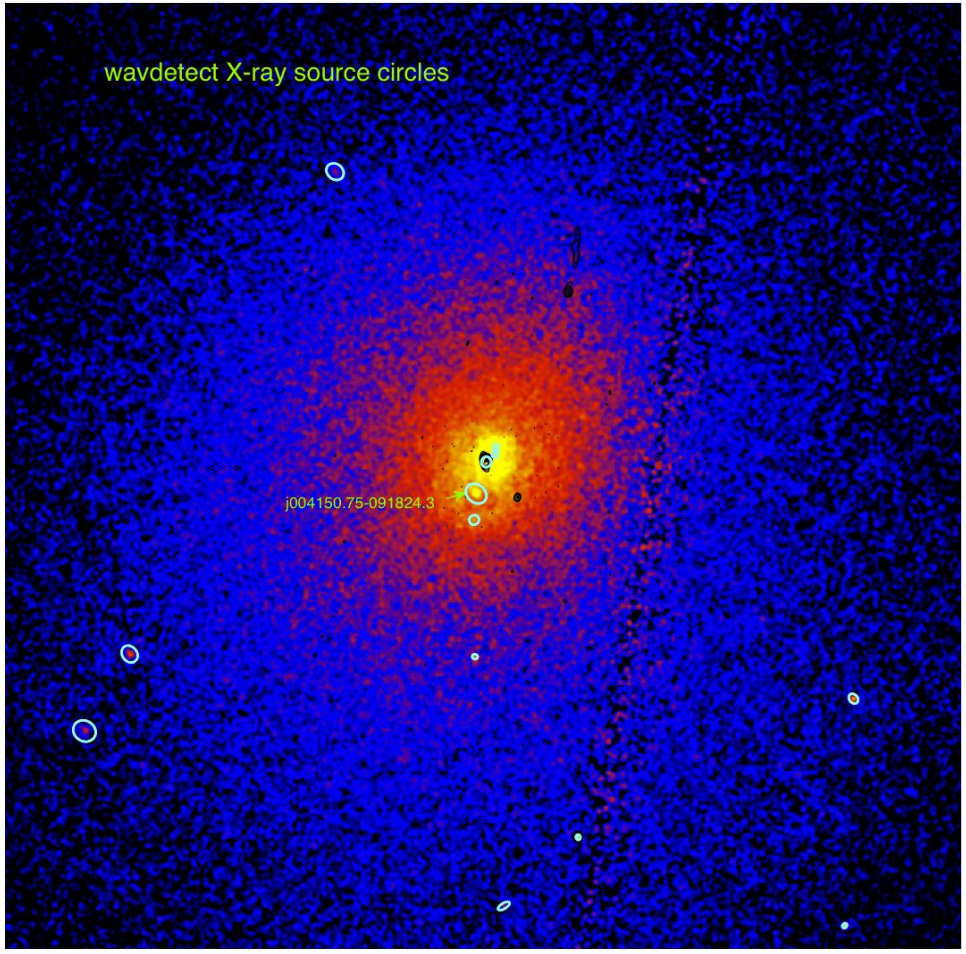


Holm 15A

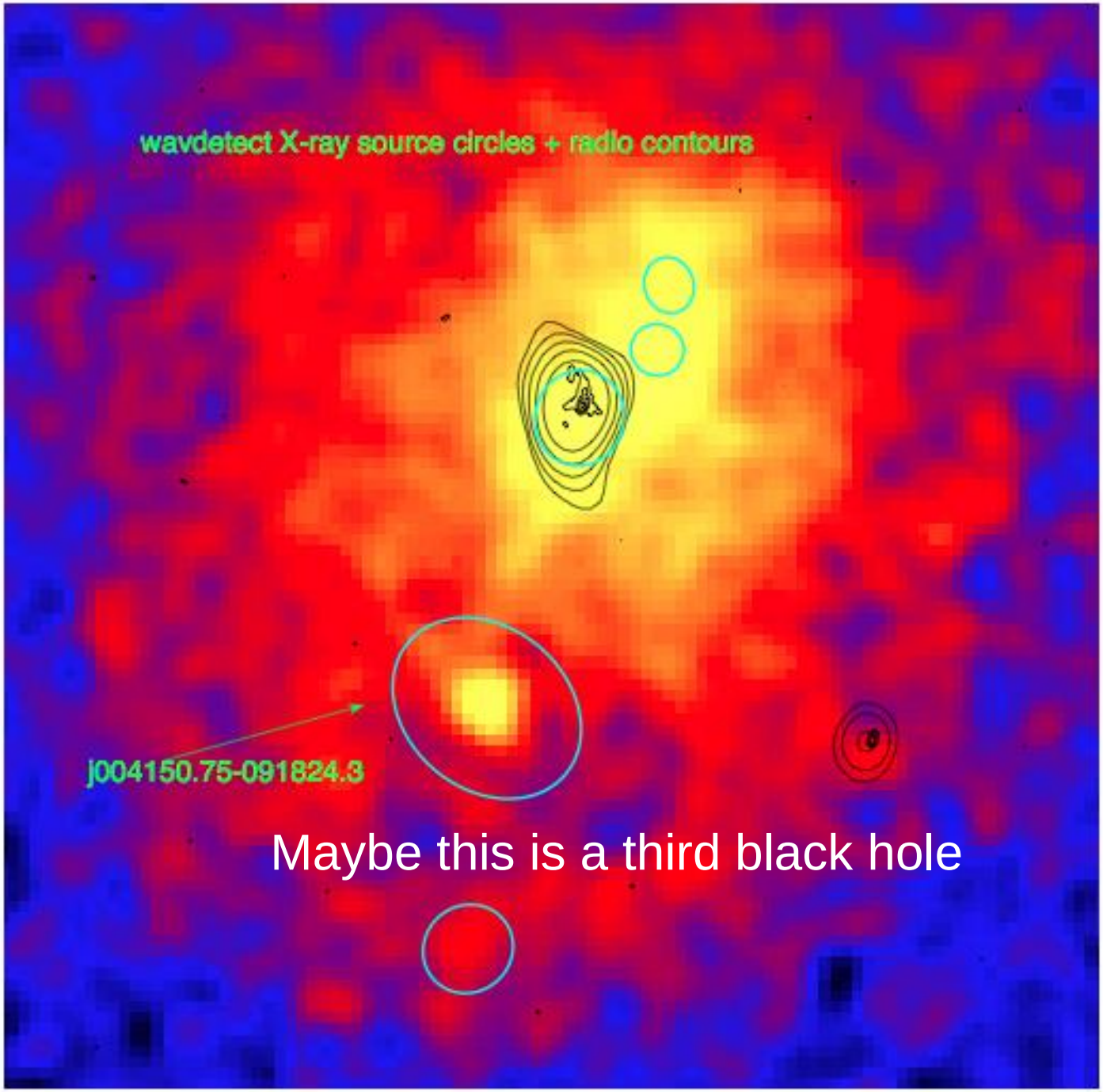


Maybe this is a third black hole

## Holm 15A

We have been granted telescope time at GTC during 2017 to confirm the membership of J004150

# WORK IN PROGRESS WITH FRANCISCO SIDDHARTA GUZMÁN MURILLO (DFM-UMSH)

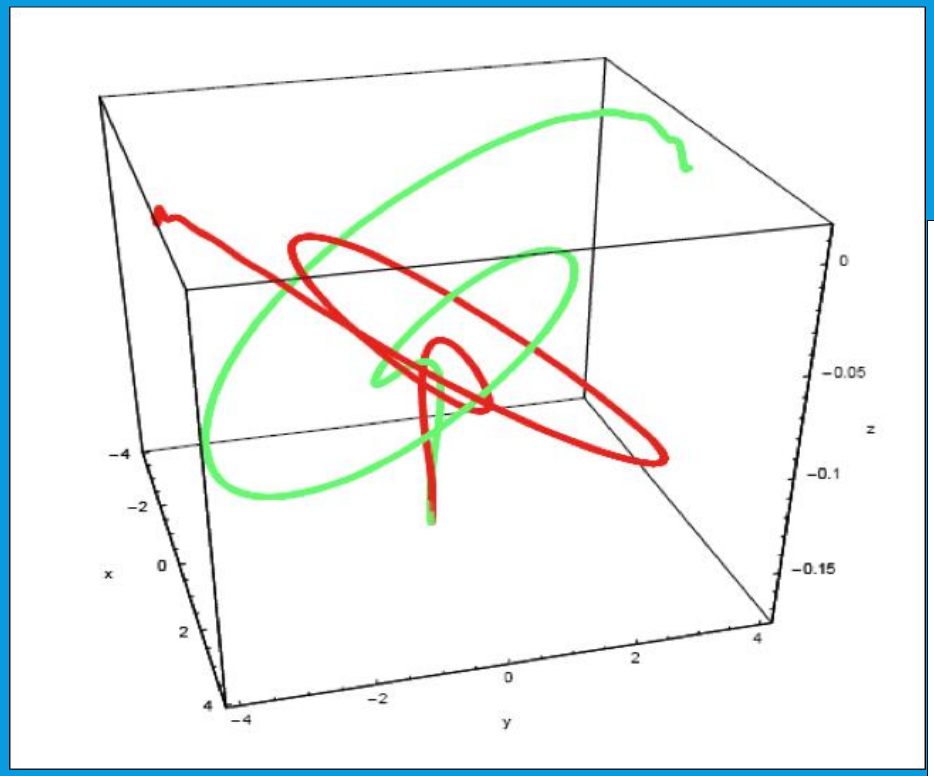


Kicked reach up to 4000 km/s Kicked $10^6$ $M_{sun}$ BH can

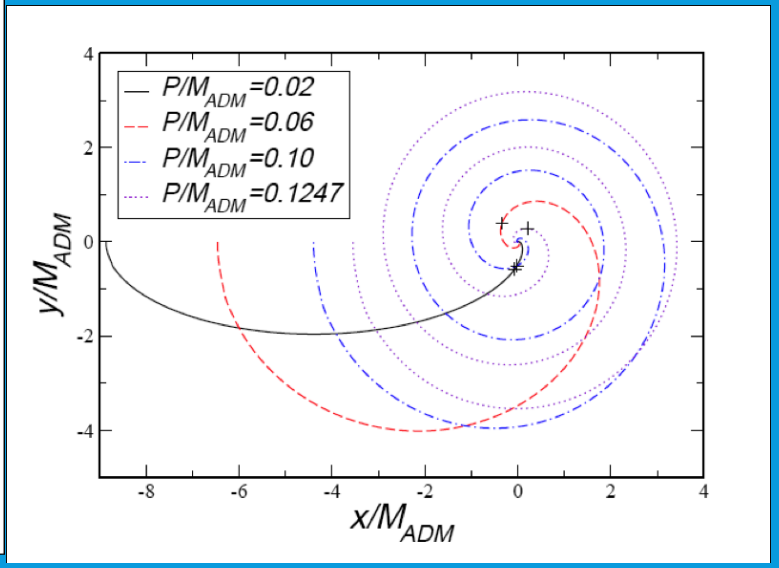

# WE NEED TO EXPLORE SCALING LAWS AT THE MOST MASSIVE END.

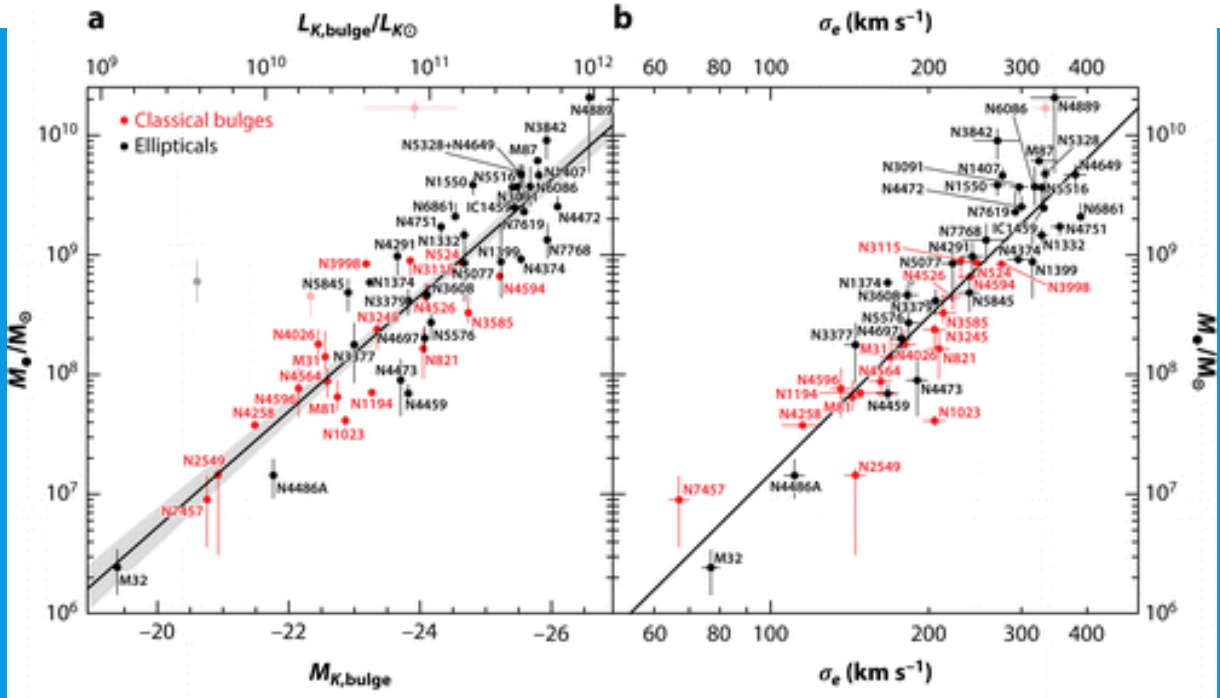


Kormendy J, Ho LC. 2013.
Annu. Rev. Astron. Astrophys. 51:511–653

$$\frac{M_\bullet}{10^9\,M_\odot} = (0.544^{+0.067}_{-0.059}) \left(\frac{L_{K,bulge}}{10^{11} L_{K\odot}}\right)^{1.22\pm0.08}$$

$$\frac{M_\bullet}{10^9\,M_\odot} = (0.310^{+0.037}_{-0.033}) \left(\frac{\sigma}{200\,\mathrm{km\,s^{-1}}}\right)^{4.38\pm0.29}$$

# WE'RE PROPOSING TO HST…

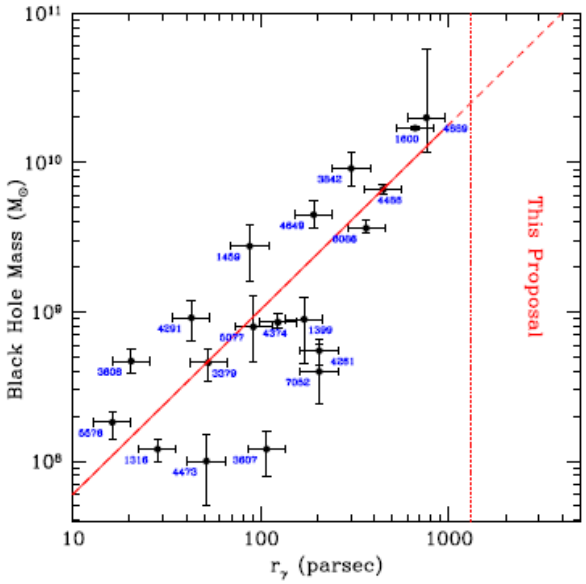


Figure 1: For elliptical galaxies with cores, black hole mass is plotted as a function
core size, $r_\gamma$ (symbols are labeled by galaxy NCG number). The red line is the $M \propto r_\gamma^{1}$
relationship that best fits the sample. No BH masses have been measured for any galax
with $r_\gamma > 1$ kpc. The $r_\gamma$ values are drawn from the Lauer et al. (2007) core sample and a
based on surface photometry derived from HST observations.

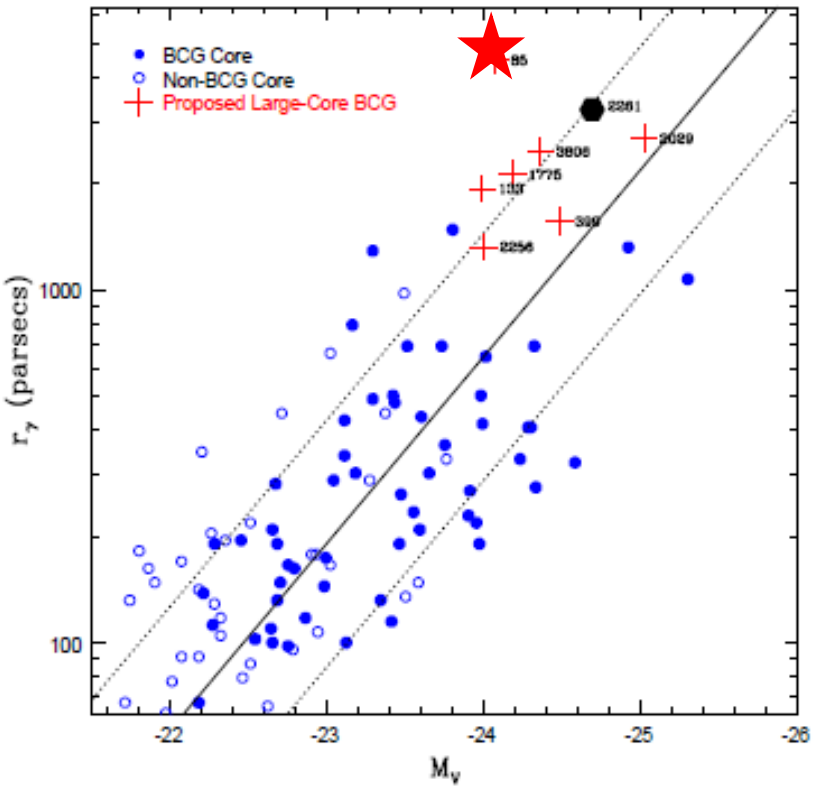

# Nature is twisted

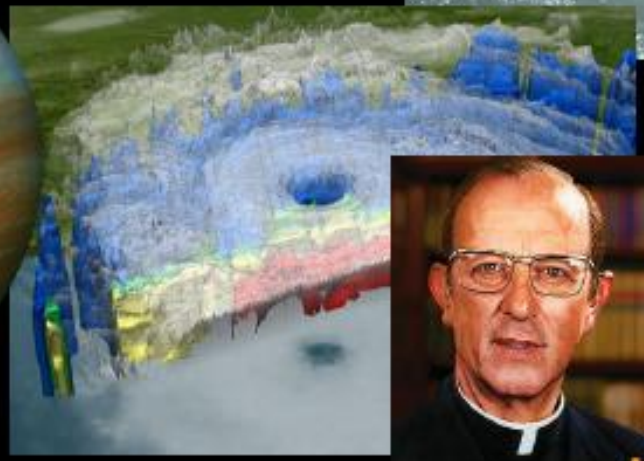

# I- Introduction

## Why Imaging?

The Planet – **Disk** Connection

* Disk **structures**, properties & FEBs
* **Dynamics** and stability
* **Early stages** of planetary formation

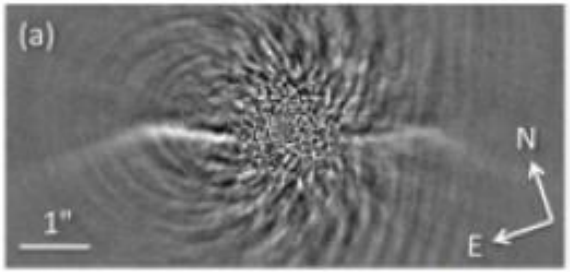


(Buenzli et al. 10)

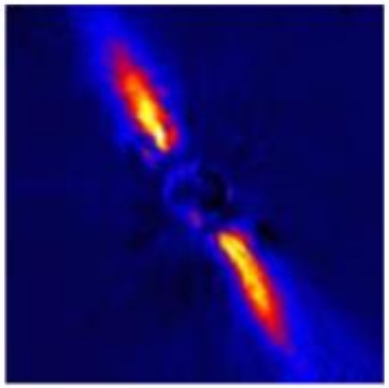

(Mouillet et al. 97)

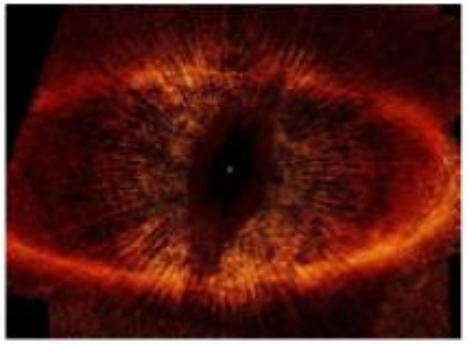

(Kalas et al. 05)

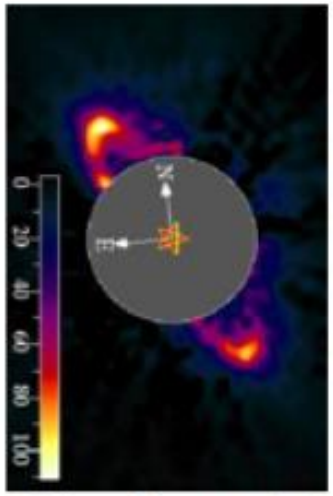

(Schneider et al. 97)

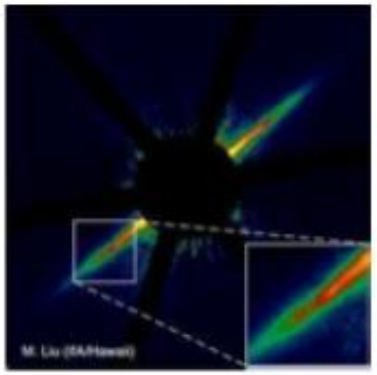

(Liu et al. 04)

Photons have spin angular momentun (s)and orbital angular momentum (OAM)

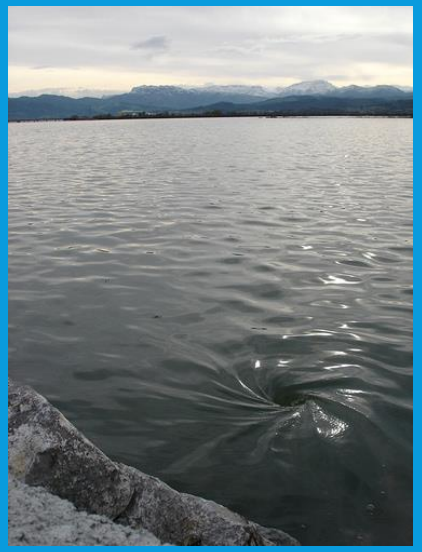

$$\mathbf{J} = \frac{1}{c^2}\int \mathbf{r}\times\mathbf{S}dV = \frac{1}{4\pi c}\int \mathbf{r}\times(\mathbf{E}\times\mathbf{H})dV$$

where $\mathbf{S}$ is the Poynting vector at $\mathbf{r}$

$$\mathbf{J} = \mathbf{J}_o + \mathbf{J}_s$$

$$\text{from QM}: \mathbf{J} = -i\hbar\mathbf{r}\times\nabla + \hbar\mathbf{s};$$

$\mathbf{s}$ is the spin matrix

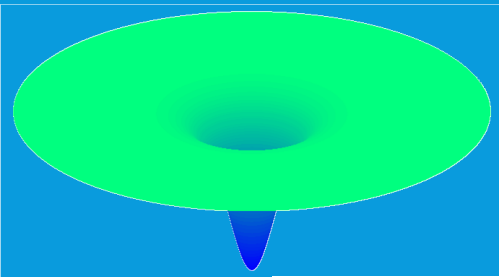

two angular momentum eigenvalue equations

$$\mathbf{J}_z E = m\hbar\mathbf{E};\ \mathbf{J}^2\mathbf{E} = \ell(\ell+1)\hbar^2\mathbf{E}$$

$$\mathbf{H}_r,\ \mathbf{E}_r = \frac{A_\ell^m S(kr)}{r(kr)^{\frac{1}{2}}} e^{iwt} P_\ell^m(\cos\theta) e^{im\phi}$$

$$|m| \le \ell$$

From Bessel

Associate Legendre Polynomial

# Martin Harwit introduced the POAM concept in Astronomy in 2003

THE ASTROPHYSICAL JOURNAL, 597:1266–1270, 2003 November 10


## PHOTON ORBITAL ANGULAR MOMENTUM IN ASTROPHYSICS

MARTIN HARWIT
511 H Street SW, Washington, DC 20024; and Cornell University, Ithaca, NY;
harwit@verizon.net
*Received 2003 April 3; accepted 2003 July 23*

### ABSTRACT

Astronomical observations of the *orbital angular momentum of photons*, a property of electromagnetic radiation that has come to the fore in recent years, have apparently never been attempted. Here I show how measurements of this property of photons have a number of astrophysical applications.

*Subject headings:* black hole physics — cosmic microwave background — extraterrestrial intelligence — instrumentation: miscellaneous — ISM: general — masers

### 1. INTRODUCTION

Photons are endowed with spin angular momentum $\pm\hbar$ along their direction of propagation. Beams of photons all carrying the same spin are circularly polarized. Less well known is that photons can also carry orbital angular momentum (OAM), $\ell$, quantized in units of $\hbar$. Curtis, Koss, & Grier (2002) have produced beams of photons each with OAM as high as $\ell = 200\hbar$.

Progress in laboratory studies of photon orbital angular momentum (POAM) has been rapid since Allen et al. (1992) first pointed out that laser—and, by inference, maser—modes with well-defined POAM can be readily produced. The characteristics of this radiation are by now reasonably well established (Allen, Padgett, & Babiker 1999; Allen

Classically, the angular momentum of an electromagnetic wave is given by the volume integral of the cross product of position $\boldsymbol{r}$ measured from the center of the multipole and the Poynting vector $\boldsymbol{S}$ at $\boldsymbol{r}$

$$\boldsymbol{J} = \frac{1}{c^2}\int \boldsymbol{r} \times \boldsymbol{S} dV = \frac{1}{4\pi c}\int \boldsymbol{r} \times (\boldsymbol{E} \times \boldsymbol{H}) dV \,. \qquad (2)$$

The same expression holds in quantum electrodynamics, but the vector field strengths now become operators acting on a state vector $\Psi$. The angular momentum $\boldsymbol{J}$ can give rise to two components that may not always be clearly separable, $\boldsymbol{J} = \boldsymbol{J}_o + \boldsymbol{J}_s$, respectively, the orbital and spin angular momenta.[1]

Quantum mechanically, one writes

# Light whirls

## Helicoidal Light Electromagnetic Waves

Figure 1

The spin angular momentum (SAM) of light is connected to the polarization of the electric field. Light with linear polarization (left) carries no SAM, whereas right or left circularly polarized light (right) carries a SAM of $\pm\hbar$ per photon.

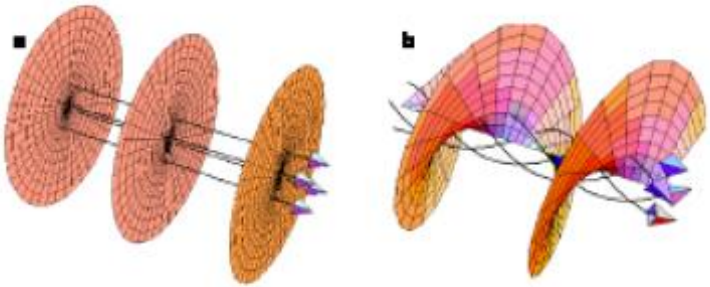

Figure 1. Laser beams usually have planar wavefronts with wavevectors parallel to the beam axis. Beams with helical wavefronts have wavevectors which spiral around the beam axis and give rise to an orbital angular momentum.

# Helicoidal waves

$$r_m = \frac{a\lambda f}{\pi\rho}\left(1 + \frac{m}{m_0}\right)$$

$m$ is called the topological charge,
$r_m$ size of the dark spot,
$f$ is the focal length,
$\rho$ radius of the optical train
$a \sim 2.585$
$m_0 \sim 9.80$

**Intensity**

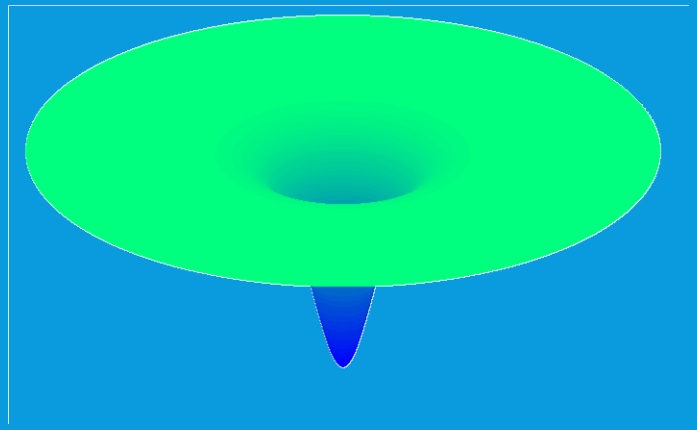

**Phase**

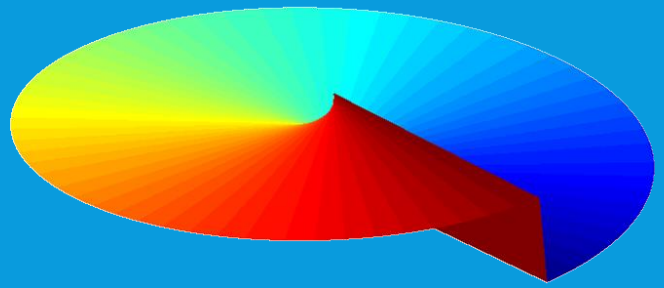

# Photon Orbital Angular Momentum (POAM)

$E(\boldsymbol{r}) \sim \exp(im\varphi) \rightarrow$ ***Rotating*** Poynting Vector $\boldsymbol{S}$

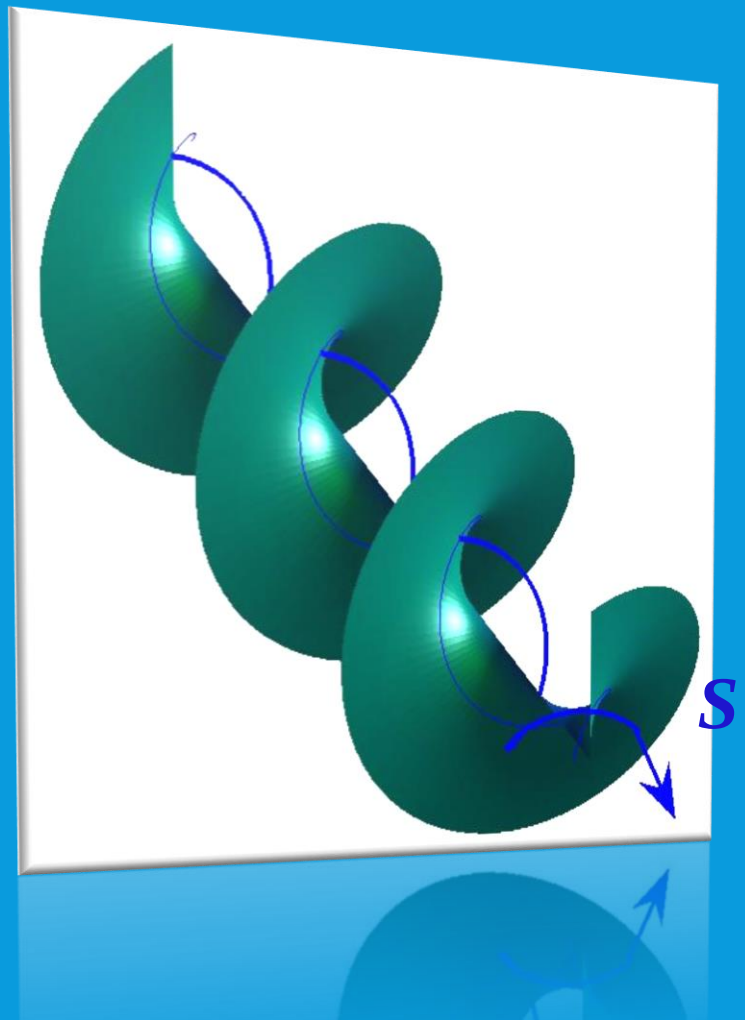


Orbital Angular Momentum:

$$J_z = m\hbar E$$

***m*** **TOPOLOGICAL CHARGE**

Allen et al., *Phys. Rev. A* **45**, 8185 (1992).

# Tamburini et al. 2011 breakthrough
# 2012, New J. Phys, 14, 033001
# Encoding many channels in the same frequency through radio vorticity: first experimental test

**Table A.2.** Azimuthal elevation required to obtain the shape of the helicoidal parabolic antenna from the initial parabolic pattern expressed in wavelength units and centimetres.

| Azimuthal angle | Elevation (in units of $\lambda$) | Elevation (cm) |
|---|---|---|
| $0-2\pi$ | 1/2 | 6.25 |
| $\pi/2$ | 3/4 | 4.69 |
| $\pi$ | 1/4 | 3.12 |
| $(3/2)\pi$ | 1/8 | 1.56 |

**Figure A.4.** The helicoidal parabolic antenna.

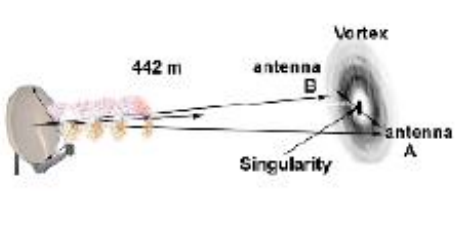


**Figure A.6.** Sketch of the experiment in San Marco (not to scale). From left to right: the transmitting antenna, the twisted radio beam and the two antennae *A* and *B* aligned with the singularity of the beam. The two receiving antennae were positioned so that the singularity was located on the baseline between the two antennae at the midpoint of the segment *AB*. Rightmost panel: schematic representation of the experiment.


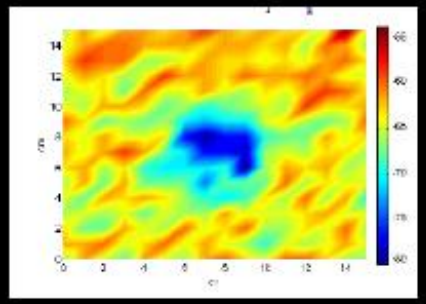

# GTM ALFONSO SERRANO SAW FIRST LIGHT AT 7MM ON DECEMBER 24TH, 2010

Dr. Alfonso Serrano Perez Grovas (1 febrero, 1950- 12 de julio, 2011)

# CORONA: 7MM RADIOMETER

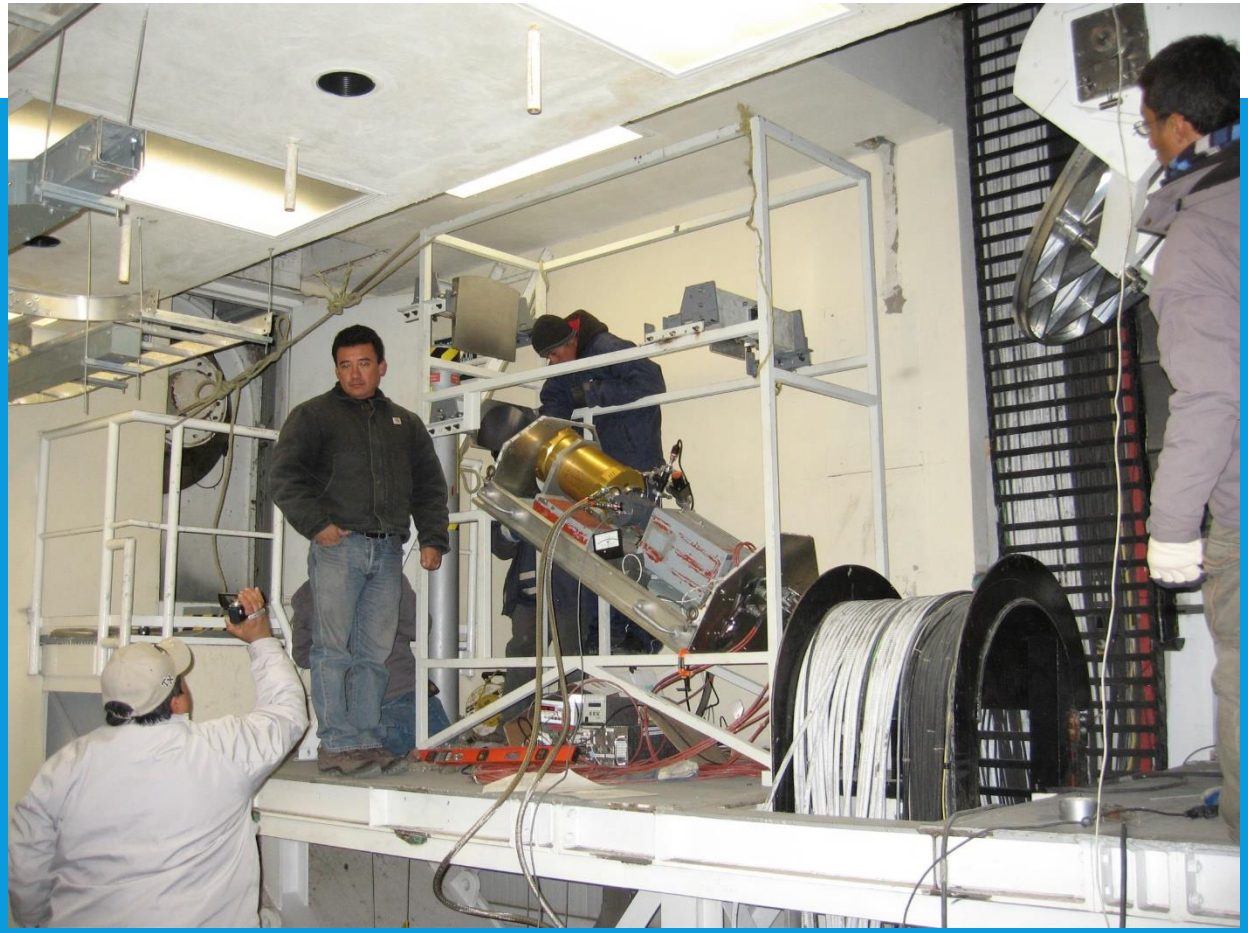

# EL GRAN TELESCOPIO MILIMÉTRICO (GTM/LMT)

Table 1: Present and future US millimeter/submillimeter facilities[a]

| Telescope | Collecting Area ($m^2$) | Frequency Range | Status |
|---|---|---|---|
| GBT | 7850 | 0.3 – 100 GHz | in operation |
| CARMA | 730 | 85 – 300 GHz | in operation |
| ARO | 79 | 85 – 500 GHz | in operation |
| CSO | 79 | 200 – 800 GHz | in operation |
| SPT | 79 | 200 – 800 GHz | in operation |
| SMA | 38 | 200 – 800 GHz | in operation |
| LMT | 1960 | 70 – 400 GHz | under construction |
| ALMA | 5650 | 85 – 900 GHz | under construction |
| CCAT | 490 | 200 – 900 GHz | in development |

[a] based on the Radio, Millimeter and Submillimeter Planning Group report for the NSF 2005 Senior Review

FOV =1.5’

Beam Size=5” (1.1mm)

Pointing accuracy= 1”

Aperture= 50m

Surface rms = 70 μm

Antenna Efficiency= 46%

180 segments

GTM/LMT will have 2-6 better brightness sensitivity than ALMA

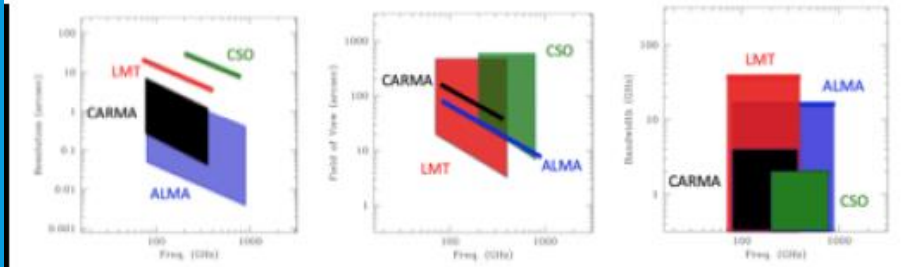


Figure 1: A comparison of angular resolution (left), field-of-view (FOV; middle), and spectral bandwidth (right) among current and future mm/smm facilities. The LMT closely matches the angular resolution of the compact configurations of interferometers like CARMA and ALMA while greatly exceeding their FOV

# SUPER-RALEIGH RESOLUTION FOR L=2

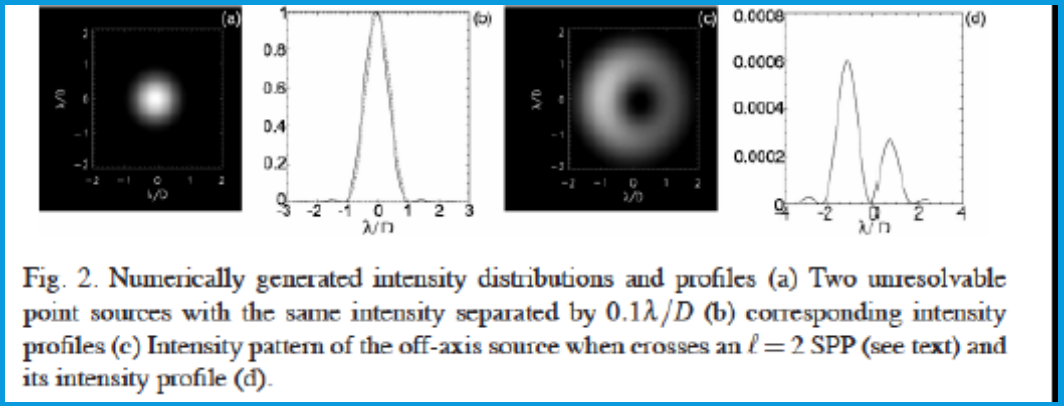


Fig. 2. Numerically generated intensity distributions and profiles (a) Two unresolvable point sources with the same intensity separated by $0.1\lambda/D$ (b) corresponding intensity profiles (c) Intensity pattern of the off-axis source when crosses an $\ell = 2$ SPP (see text) and its intensity profile (d).

Mari et al. 2012, Optics Express, 20, 2445

Better by a factor of 10

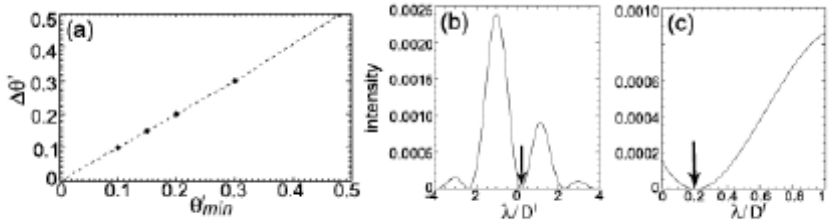


Fig. 3. (a): Plot of minima position versus angular separation. points represent numerically calculated examples. (b): Numerically generated intensity profile of one of two unresolvable point sources with the same intensity. Arrow indicate the minimum position $\theta_{min}$ for the angular separation $0.2\lambda/D'$. (c) Enlargement of the minimum zone of the profile (b). The minimum occur exactly at the angular separation $0.2\lambda/D'$.

# GRAN TELESCOPIO MILIMÉTRICO ALFONSO SERRANO PÉREZ-GROVAS (GTM/LMT) (MARCH 15, 2013)

# THE SEGMENTED VORTEX TELESCOPE CORONAGRAPH

GTM/LMT is a Cassegrain Telescope, this can be modeled as:

$$U_0(r,\phi) = T_0(r,\phi)\exp\left[-ik\left(\frac{r^2}{2f}\right)\right]e^{ikW(r,\phi)}e^{im\phi}$$

Aberration Function

In order to generate images you need to solve the Fraunhofer diffraction integral:

$$U_f(\rho,\theta) = C\int_{-\pi}^{\pi}\int_{0}^{\infty} T_0(r,\phi)e^{ikW(r,\phi)}\exp\left[i\frac{2\pi}{\lambda f}r\rho\cos(\phi-\theta)\right]r\,dr\,d\phi$$

# SVT: RESHAPING THE PRIMARY SURFACE

**Figures**

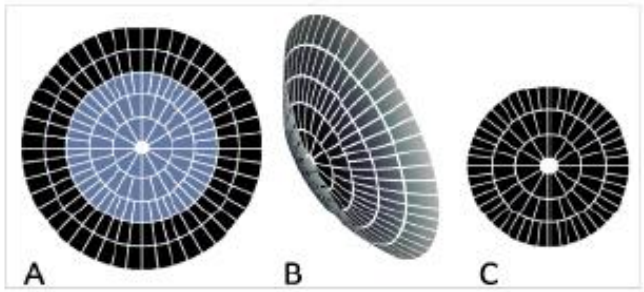


Figure 1: A: Complete setup with five rings as originally designed. Segments in black are currently not active. B: The collector mirror of the LMT/GTM generates a wavefront with this shape. The lines correspond to the gaps between the telescope segments. C: Front view of the transmittance function of the current three rings of the collector.

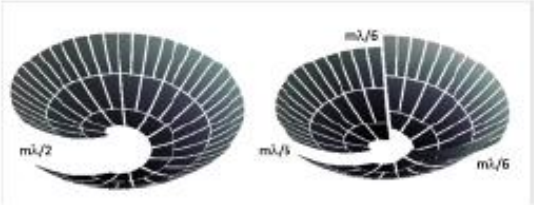


Figure 2: Multiple pitch mirror for the segmented vortex telescope.

$$\text{Maximum displacement} : \frac{m\lambda}{2}$$

$$\text{junction displacement} : \frac{m\lambda}{2}\frac{n}{N}$$

- GTM/LMT can provide us with a new ‘gallery’ for submm-bright systems, complete (from JCMT) out to 60 pc.
  - disc sizes are *not* as diverse as previously thought?
  - Use GTM/LMT as a SVT coronagraph and search for planets outside circumstellar disks for host stars beyond 60 pc (AzTEC mapping speed 0.55 deg$^2$/hr/mJy$^2$ )

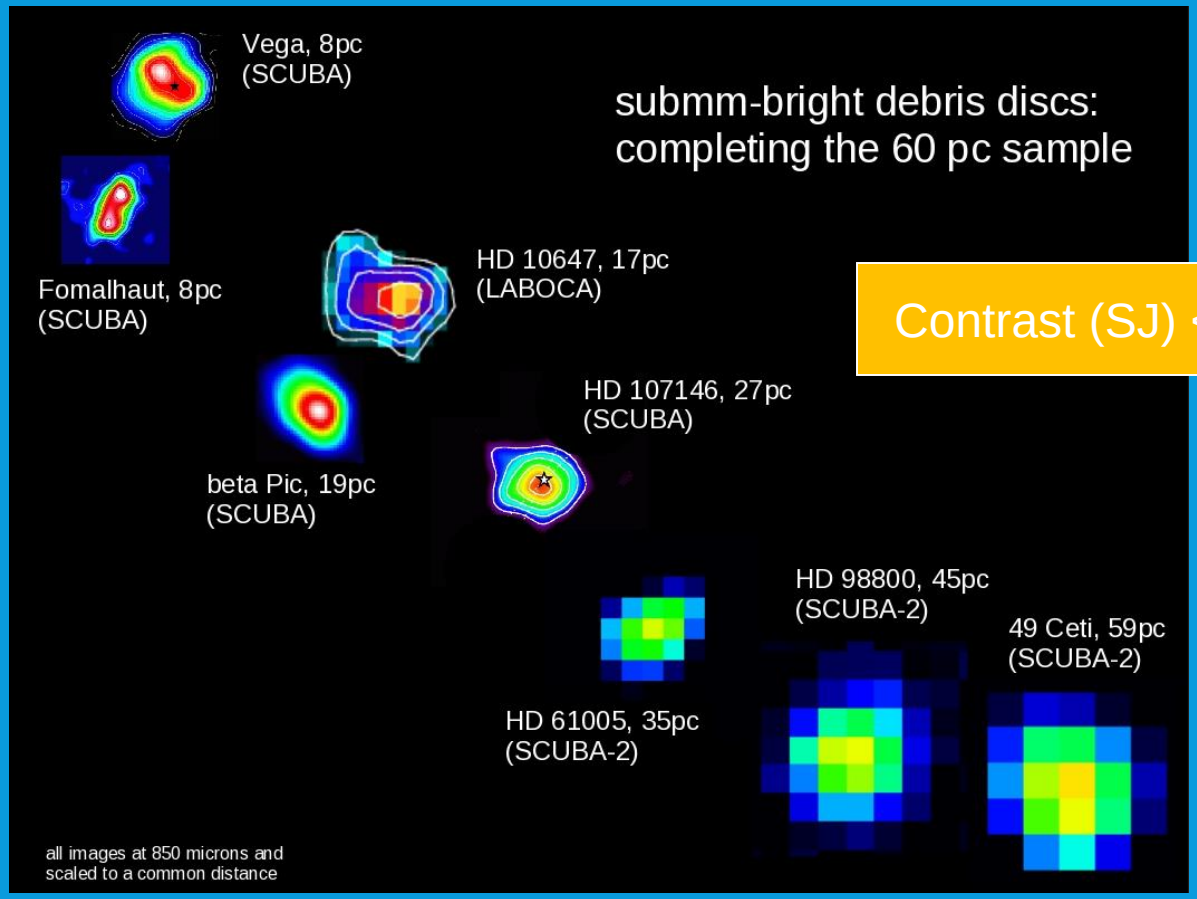

# AUGUST 2013 OPTICAL ENGINEERING'S COVER

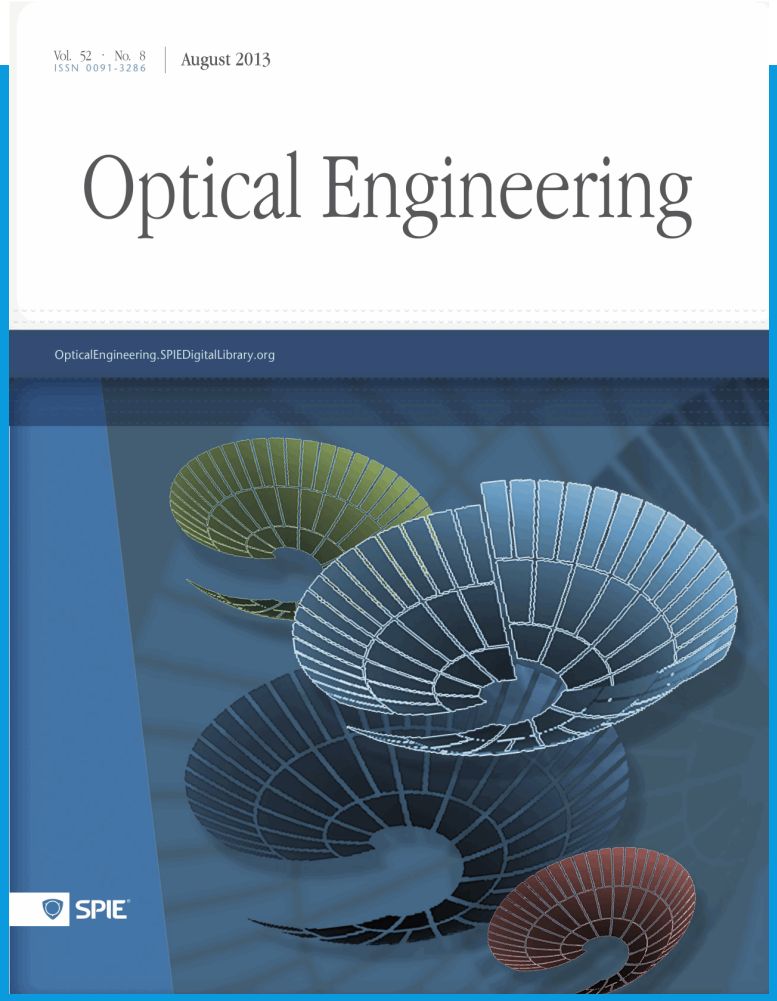


QuickTime™ and a
decompressor
are needed to see this picture.

"You have clearly done an admirably detailed feasibility study"

Sir Michael Berry, FRS
Melville Wills Professor of Physics, U. Bristol

# WHAT THE F*** HAS TO THAT VORTEX S**** WITH SMBH, AT ALL?

## Twisting of light around rotating black holes

Fabrizio Tamburini[1], Bo Thidé[2], Gabriel Molina-Terriza[3] and Gabriele Anzolin[4]

[1]*Department of Astronomy, University of Padova, vicolo dell'Osservatorio 3, I-35122 Padova, Italy, EU*
[2]*Swedish Institute of Space Physics, Box 537, Ångström Laboratory, SE-75121 Uppsala, Sweden, EU*
[3]*QuicTech and Department of Physics and Astronomy, Macquarie University, 2109 NSW Australia*
[4]*ICFO, Parc Mediterrani de la Tecnologia, Av. del Canal Olimpic s/n, ES-08860 Castelldefels (Barcelona), Spain, EU.*

**Kerr black holes are among the most intriguing predictions of Einstein's general relativity theory[1,2]. These rotating massive astrophysical objects drag and intermix their surrounding space and time, deflecting and phase-modifying light emitted nearby them. We have found that this leads to a new relativistic effect that imposes orbital angular momentum onto such light. Numerical experiments, based on the integration of the null geodesic equations of light from orbiting point-like sources in the Kerr black hole equatorial plane to an asymptotic observer[3], indeed identify the phase change and wave-front warping and predict the associated light-beam orbital angular momentum spectra[4]. Setting up the best existing telescopes properly, it should be possible to detect and measure this twisted light, thus allowing a direct observational demonstration of the existence of rotating black holes. Since non-rotating objects are more an exception than a rule in the Universe, our findings are of fundamental importance.**

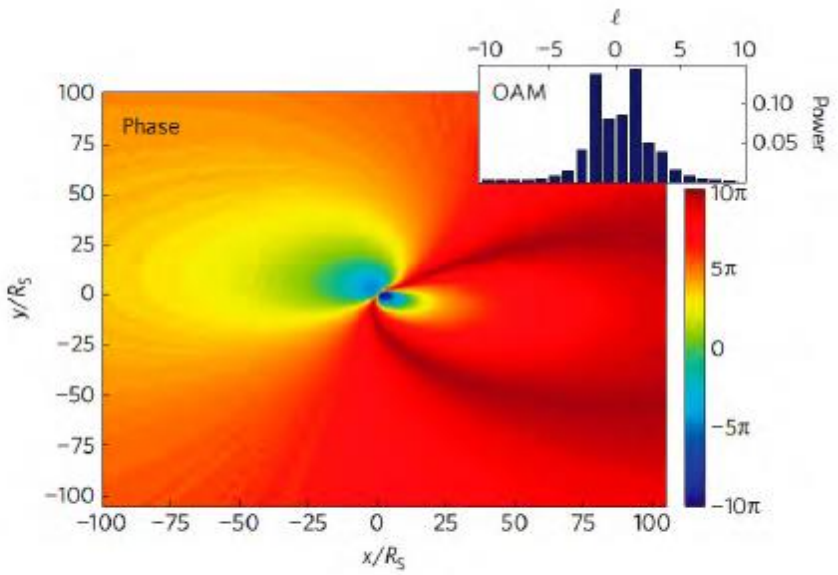


**Fig. 1**

Total phase variation of light generated in a region of 100 times 100 Schwarzschild radii ($R_s$) in the equatorial plane of a quasi-extremal rotating black hole ($a = 0.99$) as seen by an asymptotic observer located at infinity. This portion of the sky shows what would be observed with a telescope if the black hole rotation axis is inclined an angle $i = 45°$ relative to the observer. The total phase variation includes the *anamorphic* effect due to both the space-time curvature and the inclination of the disk. As shown in the right-hand panel, the corresponding OAM spectral distribution is quite complex, with two strong peaks at $\ell = -2$ and $\ell = 1$, and extends towards higher OAM modes with a rapid fall-off.

# WE ARE GETTING THERE WITH THE EHT

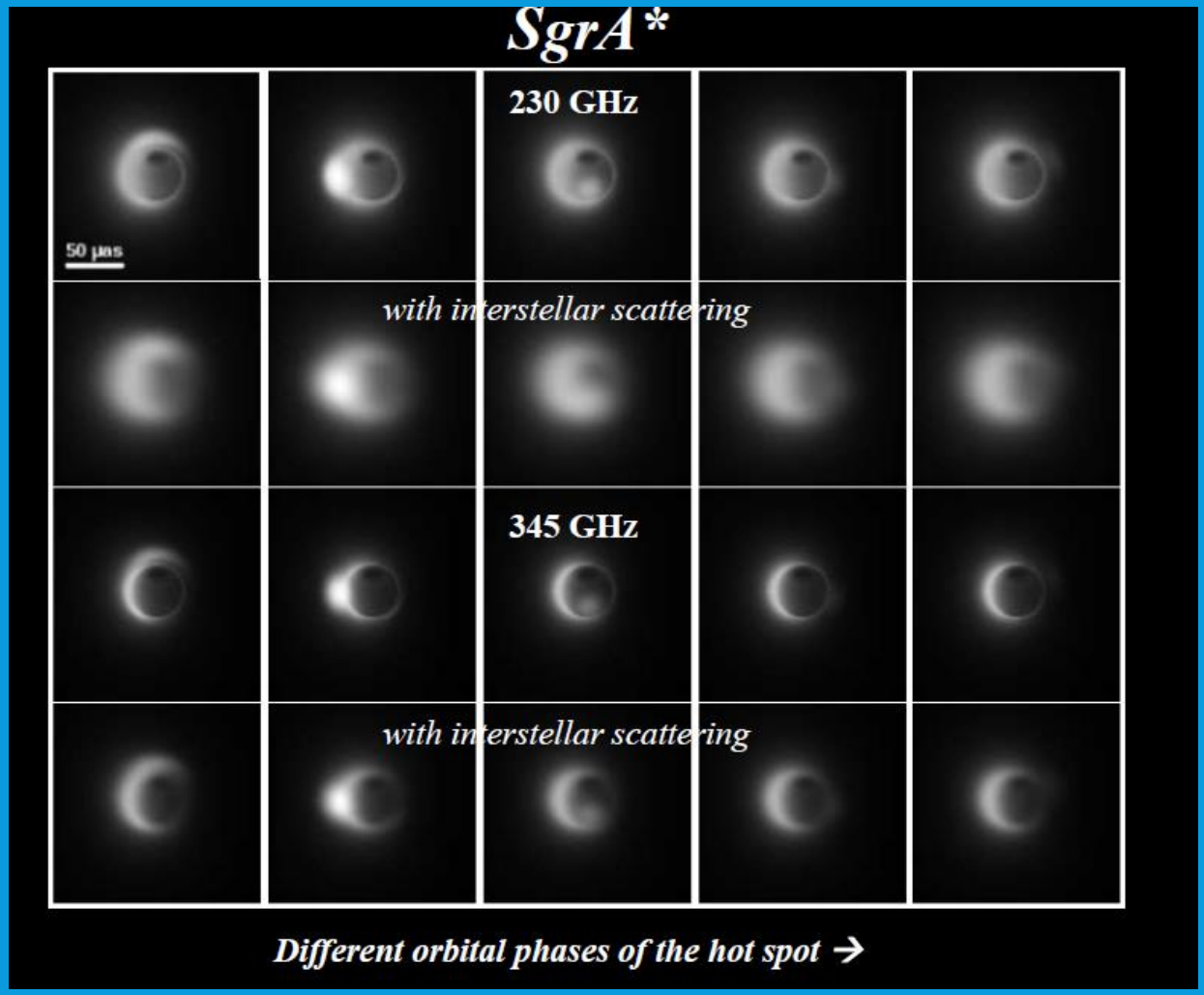

[IMAGING]

## Shooting the Beast

Astronomers are developing several radio telescope arrays to form a globe-spanning network of observatories (*right*) that can observe Sgr A* and its immediate surroundings at wavelengths near 0.87 and 1.3 millimeters—two "windows" that are not excessively absorbed by Earth's atmosphere or scattered by interstellar gas. The size of the network will permit observations with sufficient resolution to produce images of Sgr A*'s event horizon.

The appearance of Sgr A* should reveal information about the orientation of the black hole's accretion disk along our line of sight and how fast the black hole is spinning—two of the most basic facts to be learned about the Sgr A* system and vital for understanding whatever else is observed about it (*below*). On occasions when a bright spot flares up in the accretion disk, gravitational lensing by the black hole will form multiple subimages of the spot (*opposite page*). If these subimages can be resolved, they will provide detailed information about the gravitational field near the black hole, which will stringently test the predictions of general relativity.

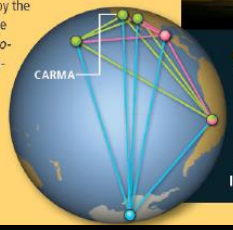


**COLLECTING DATA**
The Combined Array for Research in Millimeter-Wave Astronomy (CARMA; *above*), located at Cedar Flat, Calif., is one of several radio telescope arrays astronomers are developing to observe Sgr A*'s event horizon. A network of such observatories (*left*) separated by baselines thousands of kilometers long (*lines*) can exploit a technique called very long baseline interferometry to produce images with resolutions as fine as those that would be possible with a radio dish the size of Earth. Four arrays (*green*) are ready to be used together, two (*pink*) are under development, and the last (*blue*) needs only to be adapted for observations at submillimeter wavelengths.

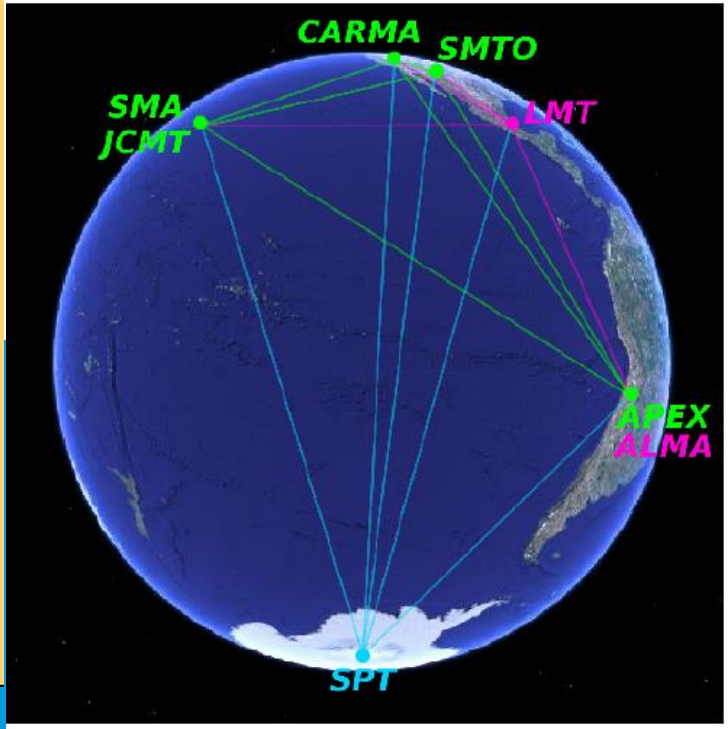


## Evidence for a Low-Spin BH in SgrA*

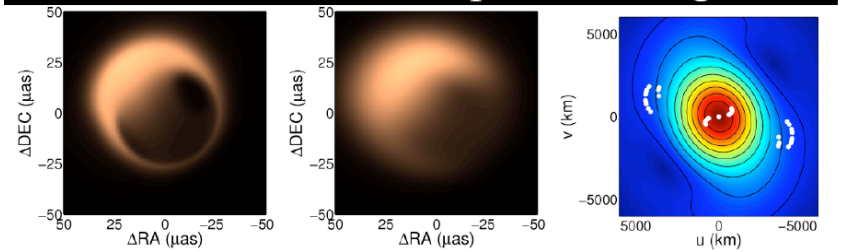


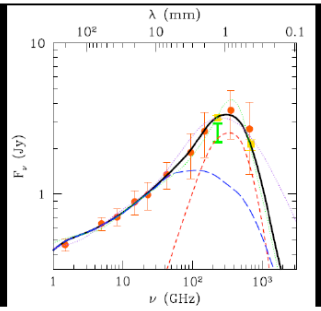


*Broderick, Fish, Doeleman & Loeb 2010*

Detecting the vortex could provide evidence that the SMBH in the center of the Milky Way is rotating…

# CAN WE CONSTRAIN THE INITIAL MASS OF SMBH?

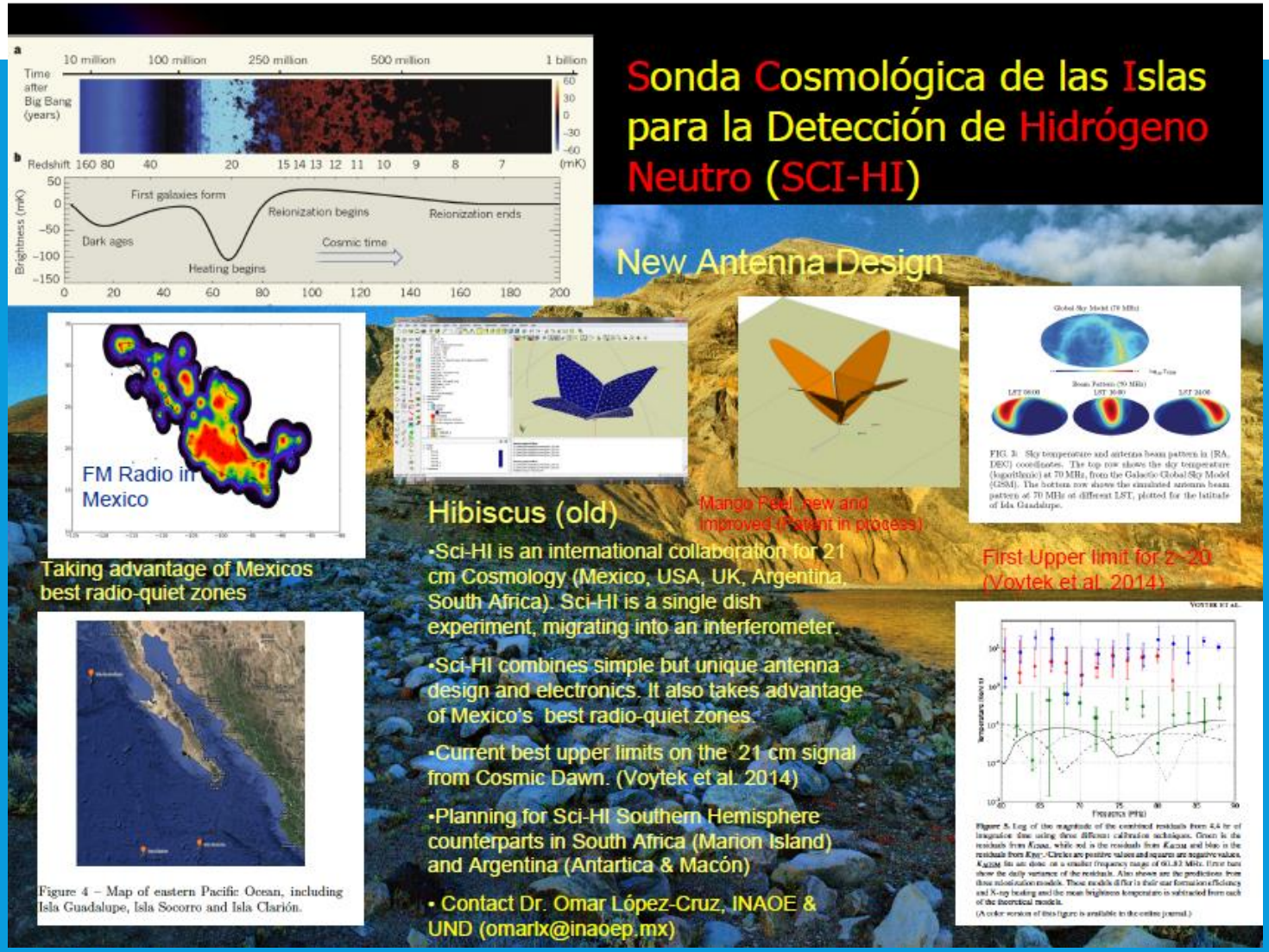

# CONCLUSIONS

Black holes are everywhere…

They have become more fundamental than we had anticipated.